Inclusive processes in high-energy hadron interactions

V. G. Grishin

Joint Institute for Nuclear Research, Dubna, Moscow District
Usp. Fiz. Nauk **127**, 51–98 (January 1979)

The general features of the multiple production of particles in high-energy hadron interactions are reviewed. The reliability of the corresponding experimental results, which are used widely in constructing theoretical models, is discussed.

PACS numbers: 13.85.Kf

CONTENTS

1. INTRODUCTION

When the new generation of proton accelerators (at Serpukhov, Geneva, and Batavia) went into operation, a systematic study of hadron interactions was begun at energies ranging from tens of GeV to 2000 GeV. The de Broglie wavelengths of the protons in these accelerators are 10^{-14}–10^{-15} cm in the center-of-mass (c.m.) system of the two nucleons, so that the structure of the interactions and the particles can be studied at distances much smaller than the "average" dimensions of the particles ($\approx 10^{-13}$ cm). Historically, as new space-time regions have become accessible to physics research, previously unknown worlds of physical phenomena have been discovered.[1,2] In line with this record, the intense experimental and theoretical research on particle interactions at $E \gtrsim 10$ GeV which was carried out from 1968 to 1978 has substantially affected our understanding of the strong interactions and hadron structure. We are thinking primarily of the discovery of a new interaction symmetry: scaling. Scaling was discovered in deep inelastic electron-nucleon interactions at high values of the energy and momentum transfer from the electron to the nucleon.[3] The essential feature of scaling is that the invariant cross sections for these reactions depend on dimensionless ratios of kinematic variables.[4-8] The scaling symmetry is thus only approximate, and it holds for $E > M$, where M represents the characteristic masses of the particles in the reactions. Scaling in the weak, electromagnetic, and strong interactions has been given a common theoretical interpretation on the basis of the quark-parton models for hadrons.[8-10] According to these models, the hadrons consist of point particles (e.g., partons), which interact and form the observable particles. These three types of interactions have thus been given a common interpretation for the first time at high energies.

It is extremely important to check the foundations of this approach, in particular, the assumptions regarding the parton properties. A unique possibility for obtaining information of this type on parton-parton interactions is presented by those hadron interactions which lead to the production of particles or "jets" with large transverse momenta ($p_\perp > 1$ GeV/c), i.e., the short-range interactions. The cross sections for these processes turn out to be many orders of magnitude larger than those expected from a simple extrapolation of the data from $p_\perp < 1$ GeV/c (Refs. 11 and 12). Another unexpected result is the success of the quark model in describing multiple production with $p_\perp \lesssim 1$ GeV/c (Ref. 13). In this case the success of the theory in classifying particles according to unitary multiplets has blended with its success in interpreting multiple processes according to the quark model. In

 0038-5670/79/010001-25$01.10

this new energy region a new world of physical phenomena is gradually taking shape, and we find that it is possible to speak in terms of the quark structure of hadrons, the unity of all types of particle interactions, etc.[1]

Most of the results for $E \gtrsim 10$ GeV have been obtained by new methods for studying particle collisions,[14,15] which are quite different from the methods used at $E < 10$ GeV. At relatively low energies, the efforts of the theoreticians and the experimentalists were concentrated on reactions with a fixed number of secondary particles ("exclusive" reactions). In those cases in which the experimentalists were not able to detect all the particles, the event was treated as a failure of some sort, and the resulting data were essentially ignored. This approach was suitable at energies at which only a few particles were produced, but in the new energy range ($E > 10$ GeV), where tens of particles are produced, this approach can no longer be used. The characteristics of one or several selected particles have been widely studied, both theoretically and experimentally.[14,15] This method, which has been labeled[8,9] the "inclusive" method,[1)] gives us much less information about the various specific reactions, but the general aspects of the interactions are seen more clearly in inclusive processes, in which the particular details are eliminated through an averaging over the characteristics of many channels and many secondary particles. It is in inclusive processes that scaling, the common features of different types of interactions, and evidence of hadron structure have been observed. There can be no doubt also that this method for studying particle interactions will remain the most important one at even higher energies.[2)]

The number of experimental and theoretical papers which have been published on inclusive processes is already huge. Some of the results have been summarized in reviews.[17-24] In Ref. 22, for example, there is a detailed discussion of scaling in strong interactions and of approximate scaling. Several theoretical modesl for multiple production of particles are reviewed in Refs. 20 and 23, so we will not discuss these questions; we will instead focus on other experimental results which are general in nature. We will attempt to determine the reliability of the various conclusions which have been drawn from experiment and which are widely used by the theoreticians in constructing their models. We will also examine the physical interpretation of the observed regularities, especially in connection with the quark model, which has been successful in explaining the basic features of hadron and hadron-nucleus interactions.

In Section 2 below we will examine the multiplicity distributions and the correlations among them. Section 3 is a brief report of a study of the two-particle rapidity and azimuthal-angle correlations. The inclusive production of resonances (Section 4) is treated in more detail, because the predominant role of these resonances in the production of secondary particles changes our understanding of the dynamics of hadron production and our understanding of the reasons for scaling violations. These resonances furnish evidence of $SU(6)$ symmetry for the strong interactions. Since this is an important question, we will include a special discussion of the experimental procedure for distinguishing resonant states and the reliability of the resulting data. In Section 4 we will also discuss the foundations of the additive quark model, (AQM) which has been successful in describing multiple-production processes in hadron and hadron-nucleus interactions.

The quark description of inclusive processes is very attractive because it allows us to discuss the weak, electromagnetic, and strong interactions from a common standpoint, on the basis of information on hadron structure.[8] At the present moment, however, we definitely do not have enough experimental information to discuss the many dynamic models of this type which are candidate theories for strong interactions for reactions in which particles with low transverse momenta ($p_\perp \lesssim 1$ GeV) are produced. We will accordingly restrict the analysis to a discussion of the symmetry properties of the quark models and their predictions for two phase-space regions [the central and fragmentation regions (Subsection 4d)]. This is the level of sophistication of the additive quark model, which gives a satisfactory explanation for the experimental data available.

In Section 5 we will examine a general method for studying the "dimensions" of the region of the secondary-particle emission on the basis of interference of identical particles, and we will discuss the experimental results obtained by this method.

Reactions in which particles with $p_\perp \gtrsim 1$ GeV/c are produced require a special review, and we will not discuss them in this paper. At the conclusion of the paper we will briefly summarize the results of the study of multiple-production processes.

2. MULTIPLICITY OF SECONDARY PARTICLES IN HADRON INTERACTIONS

The construction of theoretical models for the multiple production of particles begins with the multiplicity (n) distributions $P(n, s)$ as functions of the total c.m. energy ($\sqrt{s}$). At this point, however, we do not have data on $P(n, s)$ for a given kind of particles (π^-, K^+, p, etc.) over the entire energy range accessible in accelerators, 10–2000 GeV. Most of the data are on $P(n_{ch}, s)$ at certain energies, where n_{ch} is the number of charged secondary particles ($\pi^\pm, p, \bar{p}, K^\pm, \Sigma^\pm$, etc.), or the "charged multiplicity." Information of this type can be obtained relatively easily and quickly in bubble-chamber experiments with accelerators of the ordinary type at $n_{ch} \lesssim 20$. In a comparison of theory with experiment, it is necessary to take into account the differences in the behavior of $P(n, s)$ as a function of the energy for pions, kaons, nucleons, etc. In the

[1)] Inclusive processes have been studied for a long time in cosmic-ray physics, which furnished the first results on high-energy hadron interactions.[16-19]

[2)] Exceptional cases are elastic and diffractive processes, whose cross sections increase slowly with increasing primary energy.

models, on the other hand, it is customary to calculate $P(n, s)$ for pions, while the comparison with experimental data is based on $P(n_{ch})$. The "impurity" of heavy charged particles among the pions, however, can amount to $\approx 10\%$, and it varies with the energy.[25,26]

The distributions $P(n_{ch}, s)$ have been studied relatively well for pp interactions at momenta from 3 to 2000 GeV/c. An analysis of these data is carried out more conveniently on the basis of the s dependence of the moments of the distribution, $\langle n^k \rangle$: $\langle n^k \rangle = \sum [n(s)]^k P(n, s)$.

a. Average charged multiplicities $\langle n_{ch} \rangle$

The variation of $\langle n_{ch} \rangle$ with the energy s was the first good test of the statistical and multiperipheral models in this new energy range. These two types of models lead to different predictions regarding the behavior of $\langle r \rangle = f(s)$. The statistical models yield

$$\langle n \rangle = C_0 s^d, \tag{2.1}$$

where[20] $d = 0.25-0.5$. The scaling hypothesis and the multiperipheral models predict behavior of the type

$$\langle n \rangle = A + B \ln s. \tag{2.2}$$

If scaling does occur for the single-particle inclusive reactions

$$a + b \to c + X, \tag{2.3}$$

with an invariant cross section

$$f(x,\ p_\perp^2) = \omega \frac{d\sigma}{dp}, \tag{2.4}$$

where ω and p are the energy and momentum of particle, c and $x = p_\parallel^*/p_{max}^*$ is the Feynman variable, we have the following relationship between $f(0, p_\perp^2)$ and B:

$$B = \frac{\pi}{\sigma_{in}} \int f(0,\ p_\perp^2)\, dp_\perp^2. \tag{2.5}$$

The data on $\langle n(s) \rangle$ can thus also be used to check scaling in the central region ($x \approx 0$).

At first it appeared that there would be no particular difficulty in distinguishing between the power law in (2.1) and the logarithmic law in (2.2) over the energy range 10–2000 GeV. Consequently, the international conferences which were held in 1969–1974 featured lively discussions of the data on $\langle n_{ch}(s) \rangle$, which were the first characteristics of multiple-production reactions.

However, the situation turned out to be more complicated and ambiguous. In the first place, there were methodological difficulties in obtaining information on $\langle n_{ch} \rangle$ at the energies of the CERN ISR (Intersecting Storage Rings) experiments ($E = 300-2000$ GeV). Bubble chambers could not be used because the pp collisions occurred inside the accelerator. It was thus not until 1977 that direct data were obtained on $\langle n_{ch}(s) \rangle$, with the help of a streamer chamber.[27] Here several corrections had to be made because the apparatus did not have a complete 4π geometry, because of the stopping of slow particles in the chamber and accelerator walls, because of secondary interactions in these walls, and so forth.[27] The net result was that the systematic error in the determination of $\langle n_{ch}(s) \rangle$ was 3–5%—far worse than in bubble-chamber experiments. Figure 1 shows this experimental information on $\langle n_{ch}(s) \rangle$ as a function of P_{lab} ($s \approx 2m_N P_{lab}$) along with the data for low energies (open circles). Also shown here are the

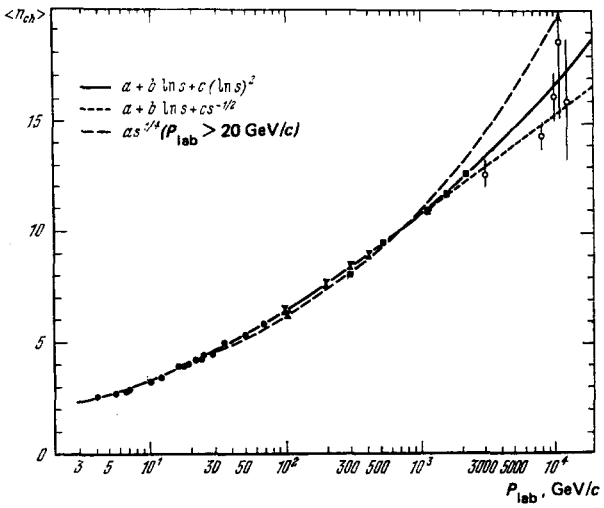

FIG. 1. Average charged-particle multiplicity as a function of p_{lab} for pp collisions.

values of $\langle n_{ch} \rangle$ obtained in cosmic-ray experiments with nuclear emulsions.[25] The best fit to all the data ($E \leq 10^4$ GeV) is achieved through the parametrization

$$\langle n_{ch} \rangle = A_1 + B_1 \ln s + C_1 (\ln s)^2, \tag{2.6}$$

where $A_1 = 0.88 \pm 0.10$, $B_1 = 0.44 \pm 0.55$, and $C_1 = 0.118 \pm 0.006$. For the more restricted energy range $\sqrt{s} \gtrsim 10$ GeV, however, both (2.2) and (2.1) also give satisfactory descriptions: $\langle n_{ch} \rangle = f(s)$ with $B = 1.5-2$ and $A \approx -1$ to -2 with $d \approx 0.2$ (Ref. 23). On the other hand, the difference in the $\langle n_i(s) \rangle$ curves is also large over this energy range[25] (Fig. 2). It follows from Fig. 2 that "threshold" effects are still important for K mesons and for $\bar{p}$, Σ, and $\bar{\Lambda}$ particles at $s \lesssim 400$ GeV^2. The cross sections for these effects grow rap-

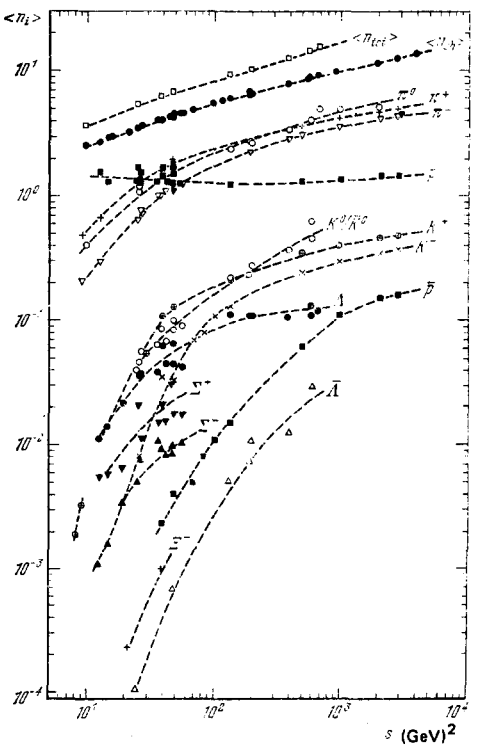

FIG. 2. Variation of $\langle n_i \rangle$ with s for pp interactions.

idly with increasing s. For pions, $\langle n(s)\rangle$ approaches a logarithmic behavior already at $s \lesssim 80$ GeV^2. As mentioned earlier, the energy dependence of $\langle n_{tot}\rangle$ and $\langle n_{ch}\rangle$ is consistent with a variation $\sim \ln s$. In a comparison of the experimental and calculated results these threshold effects must thus be into account, especially at high energies.

Thus the parameter $\langle n_{ch}\rangle = f(s)$ proved insensitive to the choice of multiple-production models in the energy range 10–10^6 GeV. Hopes for a resolution of the situation have now been transferred to the planned new accelerators with energies of 1–1000 TeV. In this energy range it will presumably be possible to distinguish between a power law and a logarithmic law (Fig. 1). Here again, however, there are methodological difficulties—the difficulties which arise at charged multiplicities $n_{ch} \gtrsim 20$. With so many particles, it becomes a serious problem to obtain data on $\langle n_{ch}\rangle$, even with hydrogen bubble chambers. A clear example of the situation is the study of $P(n_{ch})$ at energies in the range 100–400 GeV with the 76-cm hydrogen bubble chamber at the Batavia accelerator. At these energies, many of the particles are emitted in a forward cone with a half-angle $\vartheta_\pi \approx p_\perp/p_{lab} \approx 10^{-2}$ rad, so it is difficult to even count the number of particles. The situation is further complicated by the fact that for $n_{ch} \gtrsim 20$ there is an appreciable probability ($\approx 10\%$) for secondary interactions near the star ($\lesssim 5$ cm). As a result, events with $n_{ch} \gtrsim 20$ had to be processed manually already at the present-day accelerator energies, rather than by the automatic equipment used for $n_{ch} < 20$. Only after physicists analyzed the structure of the bubbles and their distribution along the track of each particle on a blown-up (9×) image of the entire event did it become possible to obtain the characteristics of events with $n_{ch} \gtrsim 20$. As the energy is raised, these difficulties will become more severe, and new methods must be developed for detecting particles with a resolution $\theta \lesssim 10^{-3}$ rad and a 4π geometry.

On the other hand, it has now been established that there is a strong deviation from scaling up to $E = 2000$ GeV (Refs. 21–23), so that the approximation of the data must begin at $p_{lab} \gtrsim 2 \cdot 10^3$ GeV. This circumstance seriously narrows the energy range of the new generation of accelerators, and it may be that the entire series of events in which $\langle n_{ch}(s)\rangle$ was used to test the model may be repeated.

To conclude this subsection we note that the first data available on $\langle n_{ch}\rangle$ in the weak, electromagnetic, and strong interactions at $E \lesssim 100$ GeV are essentially independent of the nature of the interaction, being governed by the total energy expended on hadron production.[22] It is thus necessary to study and compare the $P(n, s)$ distributions for the interactions of leptons and hadrons at accelerator energies in order to obtain information on the structure and interactions of the particles.

b. Scaling in terms of the multiplicity

If the scaling hypothesis is correct for all n-particle inclusive reactions, the multiplicity distributions are described by

$$\langle n\rangle \frac{\sigma_n}{\sigma_{in}} = \psi\left(\frac{n}{\langle n\rangle}\right), \tag{2.7}$$

i.e., depend only on the ratio $n/\langle n\rangle$ ("KNO scaling").[28] Equation (2.7) has been analyzed both in the form written here and separately for the $\langle n^k\rangle$ moments. The first comparisons of (2.7) with the experimental data yielded an excellent result: KNO scaling was observed for pp and πN interactions in the energy range 40–300 GeV (Refs. 28 and 29).

It has now been shown that an equation of the type of (2.7) with slight modifications (with n replaced by $n - \alpha$) can satisfactorily describe the $P(n_{ch}, s)$ data between 10 and 2000 GeV for the πN, NN, $\bar{N}N$, and KN interactions and also the data for collisions of hadrons with light nuclei.[21,25,30] On the other hand, it has been established that there is no scaling, even for one-particle inclusive reactions, up to $E = 2000$ GeV. In other words, the assumptions made in the derivation of (2.7) are incorrect.[21,22,28]

Accordingly in the various specific multiple-production models, the universal behavior in (2.7) is treated as the result of a random addition of the secondary particle multiplicities associated with different production mechanisms. As the energy increases, these contributions to $P(n, s)$ vary according to different laws, so that at $s > s_0$ a deviation from KNO scaling is predicted[31] ($s_0 \approx 10^6$ GeV^2).

A study of the energy dependence of the dispersion $D = \sqrt{\langle n_{ch}^2\rangle - \langle n_{ch}\rangle^2}$ has shown that the data on the pp interactions are described well by

$$D = A\,\langle n_{ch}\rangle + B = A\,(\langle n_{ch}\rangle - \alpha) \tag{2.8}$$

between 4 and 2000 GeV/c with $A = 0.57 \pm 0.01$, $B = -0.54 \pm 0.02$, and $\chi^2_{n.d} = 1.6$ (Fig. 3).[3),25] The two-component model yields a simple interpretation[32] of

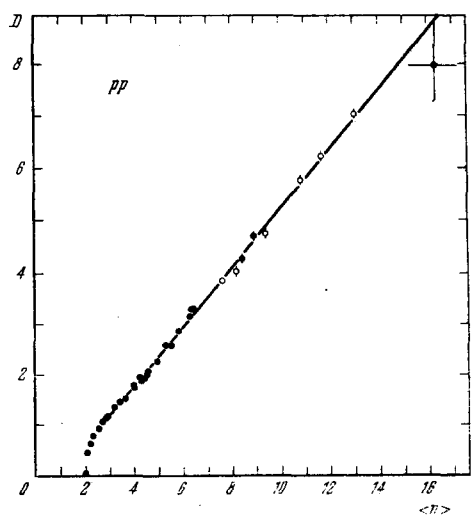

FIG. 3. Dispersion as a function of $\langle n\rangle$ for pp collisions.

[3)]Equation (2.7) can be replaced by the equivalent set of equations $\langle n^k\rangle = C_k\,\langle n^k\rangle$, where $k = 2, 3, 4, \ldots$; in the case of KNO scaling, $C_k(s) = \text{const}$. The replacement of n by $n - \alpha$ leads to equations like $\langle (n-\alpha)^k\rangle = C^k\langle n-\alpha\rangle^k$, from which, with $k = 2$, we obtain (2.8).

(2.8). In this case, the slope A is determined by the ratio of the probabilities p_1 and $p_2 = 1 - p_1$, which correspond to nondiffractive and diffractive processes, respectively ($A = \sqrt{p_2/p_1}$). Another interpretation has been offered by Buras *et al.*,[30] who suggest that the parameter α is equal to the average number of charged leading particles. Table I shows the values of the parameters A, B, and α for the pp, $\pi^{\pm}p$, $K^{\pm}p$, and $h^{\pm}n$ interactions, found[25] by approximating the data by (2.8). For all the interactions, the values of A turn out to be essentially the same ($A \approx 0.55 \pm 0.02$). The parameter α differs for the interactions of hadrons with a neutral target [$\alpha(n) = 0.46$], with the implication that this parameter can be interpreted as the average number of charged leading particles.[30] The parametrization in (2.8) yields the asymptotic values of other parameters which are related to the second moments, $\langle n_{ch}^2 \rangle$, and which are widely used to analyze the experimental data.[25] For example,

$$\frac{\langle n \rangle}{D} = \frac{1}{A}\frac{\langle n \rangle}{\langle n \rangle + B/A} \xrightarrow[s\to\infty]{} \frac{1}{A} \approx 1.73, \tag{2.9}$$

$$C_2 = \frac{\langle n^2 \rangle}{\langle n \rangle^2} = 1 + A^2 + \frac{2AB}{\langle n \rangle} + \frac{B^2}{\langle n \rangle^2} \xrightarrow[s\to\infty]{} 1 + A^2 \approx 1.33. \tag{2.10}$$

At the CERN ISR energies, these parameters differ from their asymptotic values by only a few percent[25,27] (Fig. 4). The energy behavior of the other moments of the multiplicity distribution is discussed in Refs. 25 and 27.

c) Multiplicity correlations

In Subsections a) and b) above we have been discussing the $P(n_{ch})$ distributions for the $\pi^{\pm}$ and $K^{\pm}$ mesons and charged baryons. The universal behavior which has been observed corresponds to the $\pi^{\pm}$ mesons, of course, since there are relatively few other particles ($\lesssim 10\%$). To obtain a better understanding of this general behavior, however, and to study the particle-production dynamics, we would of course need "pure" data for each particle species over the entire range of accelerator energies. At present, data of this type are available only for certain primary-particle energies.

A study of the joint production of charged and neutral pions, $P(n, n_0)$, has yielded

$$\langle n(\pi^0) \rangle = \beta n_- + \gamma, \tag{2.11}$$

where $\beta \approx 0.3$ for n^-p, n^-n, and $\pi^{-12}C$ interactions at[33-35] $p = 40$ GeV/c. At present these correlations are being studied at energies from 5 to 1500 GeV for the πN, KN, NN, and pp interactions. The values of β vary from -0.116 ± 0.05 to 0.89 ± 0.06 in this energy range and are essentially independent of the nature of the primary particle. The negative values of β at low energies result from energy and momentum conservation. Analogous correlations have now been established for the K_s^0 mesons which are produced in pp collisions at[36] $E_p = 100$–300 GeV. The values found for β are $\beta(K_s^0) = 0.057 \pm 0.004$, as expected on the basis of the condition $\beta(K_s^0) = \beta(\pi^0) \times \langle n(K_s^0) \rangle / \langle n(\pi^0) \rangle$ and condition (2.11). The multiplicity correlations of the type in (2.11) are thus general in nature, and it seems worthwhile to pursue their study. Equation (2.11) can be interpreted either according to the model of independent cluster (resonance) production[37] or by taking into account branching in the multiperipheral approach at $p_T \gtrsim 20$ GeV/c (Ref. 38).

TABLE I. Values of the coefficients A, B, and α for various reactions.

Reaction	Energy range, GeV	A	B	α
pp	4—2070	0.57 ± 0.01	-0.54 ± 0.02	0.94
π^+p	7—100	0.55 ± 0.02	-0.61 ± 0.06	1.11
K^+p	8—100	0.53 ± 0.04	-0.46 ± 0.14	0.87
π^-p	20—360	0.56 ± 0.01	-0.58 ± 0.07	1.04
K^-p	32—147	0.53 ± 0.09	-0.32 ± 0.43	—
$h^{\pm}n$	5—300	0.58 ± 0.02	-0.27 ± 0.05	0.46

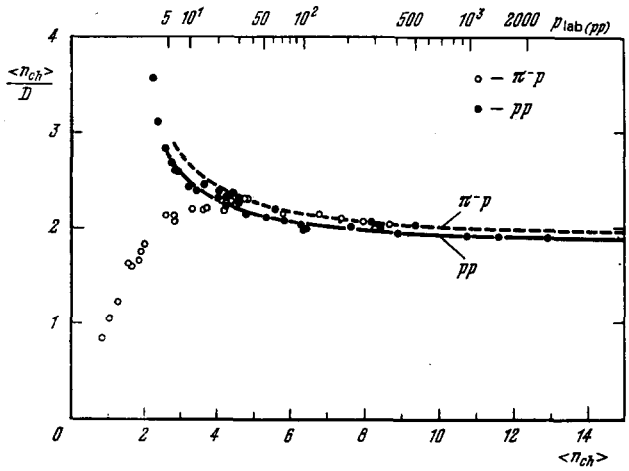

FIG. 4. The ratio $\langle n_{ch} \rangle / D$ as a function of n_{ch} for pp and π^-p interactions. The curves are calculations using the equation $D = A\langle n_{ch} \rangle + B$.

In summary, a decade of work on hadron interactions in large accelerators has revealed universal regularities in multiplicity distributions, which are essentially independent of the nature of the primary particles [see (2.6)–(2.8) and (2.11)]. There are indications that these regularities are also valid for the weak and electromagnetic interactions,[39] but at this point we have no data on $P(n_i)$ and $P(n_i, n_k)$ at accelerator energies for different types of secondary particles, so it is difficult to interpret the observations theoretically. The program of experimental research on multiplicities is thus far from completion.

3. TWO-PARTICLE CORRELATIONS AMONG THE SECONDARY PARTICLES

A study of the secondary-hadron multiplicity was the first stage in the study of many-particle processes at high energies (Section 2). An equal effort has been devoted to the one-particle inclusive reactions

$$a + b \to c + X \tag{2.3'}$$

in the accelerator energy range, in order to test the scaling hypothesis for strong interactions[8-10]:

$$\lim_{s\to\infty} f'(x, p_\perp^2, s) \to f(x, p_\perp^2). \tag{3.1}$$

Although data on (2.3) have been obtained only at certain primary energies, and frequently in different x and $p_\perp$ intervals, it has now been established that the invariant cross sections in (2.3) with $x = 0$ increase with

increasing energy up to[40] $E_p = 2000$ GeV. For π^+ mesons, for example, the ratio

$$\bar{R}(\pi^+) = \frac{\sigma(63\,\text{GeV})}{\sigma(23\,\text{GeV})} = 1.36 \pm 0.02 \tag{3.2}$$

has been found for the interval $p_\perp = 40$–400 MeV/c and $x = 0$ (Ref. 40). As the mass of the secondary particles increases, $\bar{R}$ in (3.2) also increases: $\bar{R}(K^+) = 1.52 \pm 0.08$, $R(K^-) = 1.69 \pm 0.08$, and $R(\bar{p}) = 1.84 \pm 0.06$. An exceptional case is that of protons, for which $\bar{R}(p) = 1.08 \pm 0.05$, and this exception is probably due to the presence of fragmentation protons in the region $x \approx 0$ at low energies ($\sqrt{s} = 23$ GeV). It is also interesting to note that a violation of scaling can result from the intense production of resonances and their decay into pions (Section 4). In summary, an important violation of scaling, (3.1), has been found in the central region ($x = 0$) for the long-lived secondary particles[4)] ($\pi, K, \bar{N}$).

The reason for the violation of scaling is not yet clear; it may lie in the dynamics of the hadron interactions at $E_p \lesssim 2000$ GeV, but it may also lie in the kinematics of the production and decay of resonances (Section 4). In the primary-particle fragmentation region, $|x| \lesssim 1$, scaling holds within 5–10% for exotic processes even at low energies ($E \gtrsim 10$ GeV). The approach to scaling has been reviewed in detail elsewhere.[21,22]

The one-particle inclusive distributions are of course associated with hadron-production mechanisms, but since these distributions constitute the results of an averaging process, they can be described satisfactorily by a broad range of models, ranging from multiperipheral to hydrodynamic.[23] More detailed information can be acquired by studying the many-particle correlations among the secondary particles. Most of the data of this type now available are for reactions of the type

$$a + b \to c_1 + c_2 + X. \tag{3.3}$$

In this section we will discuss the main features of the reactions (3.3) and their interpretation according to the multiperipheral models incorporating cluster production. These models combine the basic features of the multiperipheral and statistical approaches.[23,41-43]

a. Rapidity correlations

Correlation data on the secondary particles are usually analyzed with correlation functions of the type

$$C_2(y_1, y_2, s) = \rho_2(y_1, y_2, s) - \rho_1(y_1, s)\,\rho_1(y_2, s), \tag{3.4}$$

where

$$\rho_2 = \frac{f_2(y_1, y_2, s)}{\sigma_{in}}, \quad \rho(y, s) = \frac{f(y, s)}{\sigma_{in}}$$

and

$$y = \frac{1}{2} \ln \frac{\omega + p_\parallel}{\omega - p_\parallel} \tag{3.5}$$

is the longitudinal rapidity of the particle.[21-23]

Integrals of the correlation functions $C_2(y_1, y_2, s)$ over the entire phase volume are expressed in terms of the moments of the multiplicity distributions. For example,

$$C_2(s) = \langle n_1 n_2 \rangle - \langle n_1 \rangle \langle n_2 \rangle \quad (c_1 \neq c_2) \tag{3.6}$$

and

$$C_2(s) = \langle n(n-1) \rangle - \langle n \rangle^2 = D^2 - \langle n \rangle \quad (c_1 \equiv c_2), \tag{3.7}$$

where n is the number of secondary particles of a given type.

The correlation functions have a simple physical meaning in the limit $s \to \infty$. If the particles are produced independently, then $C_2 = 0$. Energy and momentum conservation at finite energies, however, leads to values $C_2 \neq 0$, so kinematic correlations must be evaluated (preferably eliminated) in the data analysis.

In addition to the C functions the functions

$$R(y_1, y_2, s) = \frac{C(y_1, y_2, s)}{\rho(y_1, s)\,\rho(y_2, s)} \tag{3.8}$$

are also used. These functions are less sensitive than $C(y_1, y_2, s)$ to errors in the determination of the total number of interactions or σ_{in}.

Data are now available on the R and C functions for pp interactions at energies from 10 to 2000 GeV and on $\pi^\pm p$ interactions for $E_\pi = 10$–360 GeV (Refs. 44–49). For $E \gtrsim 30$ GeV, the basic features of the correlation effects vary only slightly with the energy, so it is sufficient to discuss the experiments at $E = 40$ GeV, for which the most thorough analysis has been made of the two-particle correlations of the charged particles and γ rays in the $\pi^- p$ and $\pi^- n$ interactions.[48] The results have been compared with phase-volume calculations and calculations based on the multiperipheral cluster model.[41-43] The phase-volume calculations incorporate the experimental multiplicity distributions (for the charged and neutral secondary particles) and energy and momentum conservation. When the results are compared with experiment, the effect of the conservation laws can be evaluated. An important feature of the multiperipheral model is that it incorporates the production of clusters, whose decay is described by the statistical theory.[23] The calculations from the multiperipheral model have been represented as an ensemble of computer-generated simulated events, so that comparison with experiment is greatly simplified. At high energies, at which many particles are produced, a comprehensive test of any model would require taking this approach, i.e., obtaining an ensemble of "theoretical" events in the same form as the experimental events. Then any distribution of interest could be extracted from both theory and experiment in a few minutes with a computer.

The situation is illustrated by Fig. 5, which shows values of $R_{ch,ch}(y_1, y_2)$ (for brevity we will henceforth write simply $R_{c,c}$) for the inclusive reactions

$$\pi^- + p \to \pi^\pm + \pi^\pm + X \tag{3.9}$$

for $p = 40$ GeV in the intervals $|\Delta y_1| \lesssim 0.8$ and $|\Delta y_2| \lesssim 2.4$ (Ref. 48). The dashed curves show the results of the phase-volume calculations; these results do not agree with experiment in the central region ($|\Delta y| \lesssim 1$). The negative values of $R_{c,c}$ at the extreme values of y are consequences of energy and momentum conservation.

[4)] This is a good illustration of the insensitivity of the functional dependence $\langle n_{ch}(s) \rangle = f(s)$ to the various models (Subsection 2a).

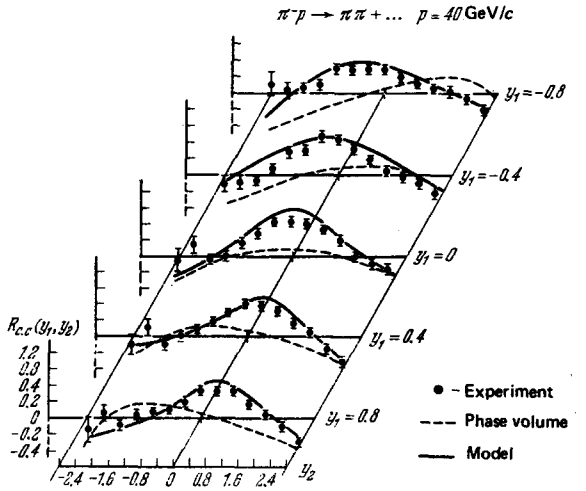

FIG. 5. Values of $R_{c.c.}(y_1, y_2)$ for $\pi^- p \to \pi\pi X$ processes at $p = 40$ GeV/c.

The experimental data are described within 5–10% by the model (the solid curves). We find a similar behavior for the R_{ik} (or C_{ik}) functions for various combinations of secondary pions and γ rays.

Analysis of the data from the energy range 30–2000 GeV yields the following conclusions.

1) The shapes of the $R_{ik}(y_1, y_2)$ and $C_{ik}(y_1, y_2)$ curves for different types of secondary particles are similar and vary only slightly with the energy. In the central region ($|\Delta y| \lesssim 2$), the $C(R)$ functions can be approximated satisfactorily by $\exp(-|\Delta y|^2/L^2)$ or $\exp(-|\Delta y|/L)$ with $L \approx 2$, where L is the correlation length. Long-range correlations ($\Delta y > 2$) have also been observed.[23]

2) The values of the $R(C)$ functions vary rapidly with increasing $|\Delta y|$ and slowly with $Y = y_1 + y_2$.

3) $R_{+-}(0, 0) \approx 2R_{--}(0, 0)$ and $R_{c.c}(0, 0) \approx R_{c.\gamma}(0, 0)$.

4) Over the energy range 40–200 GeV, the values of $R_{ik}(0, 0)$ are essentially constant and are independent of the nature of the primary particles ($\pi^{\pm}, p$):

$$\overline{R}_{c.c}(0, 0) = 0.59 \pm 0.04, \quad \overline{R}_{+-}(0, 0) = 0.74 \pm 0.15,$$
$$\overline{R}_{--}(0, 0) = 0.35 \pm 0.03, \quad \overline{R}_{++}(0, 0) = 0.23 \pm 0.05\ ^{5)}.$$

Short-range correlations of the secondary particles have thus been observed in the central region for the inclusive reaction (3.3). A possible reason for the large value of $R_{+-}(0, 0)$ in comparison with $R_{--}(0, 0)$ is the production of ρ mesons (Section 4). Estimates from data on the $R(C)$ functions lead to an average of two or three charged particles per cluster.[23] On the other hand, a study of the $R^n(C^n)$ functions in semi-inclusive reactions, in which the number of charged secondary particles (n) is fixed, shows that the situation is more complicated.

The correlation functions for semi-inclusive reactions are defined[6)] by analogy with (3.4) and (3.8):

$$C_2^{(n)}(y_1, y_2) = \rho_2^{(n)}(y_1, y_2) - \rho_1^{(n)}(y_1)\rho_1^{(n)}(y_2) \qquad (3.10)$$

and

$$R_2^{(n)}(y_1, y_2) = \frac{C_2^{(n)}(y_1, y_2)}{\rho_1^{(n)}(y_1)\rho_1^{(n)}(y_2)}, \qquad (3.11)$$

$$\rho^{(n)}(y) = \frac{1}{\sigma_n}\frac{d\sigma_n}{dy}, \qquad (3.12)$$

where σ_n is the cross section for the production of n charged particles. The C_2 and $C_2^{(n)}$ functions are related by

$$C_2(y_1, y_2) = \sum_n \alpha_n C_2^{(n)}(y_1, y_2) + G(y_1, y_2), \qquad (3.13)$$

$$G(y_1, y_2) = \sum_n \alpha_n [\rho_1^{(n)}(y_1) - \rho_1(y_1)][\rho_1^{(n)}(y_2) - \rho_1(y_2)], \qquad (3.14)$$

where $\alpha_n = \sigma_n/\sigma_{in}$.

It follows from (3.13) that the absence of dynamic correlations between pairs of particles ($C_2^{(n)} = 0$) would not imply $C_2(y_1, y_2) = 0$. In this case the correlation in the inclusive processes can be linked to the difference between $\rho^{(n)}(y)$ and $\rho(y)$, i.e., to the different mechanisms operating to produce the particles at the different multiplicities.[7)] It is thus necessary to analyze the semi-inclusive reactions in order to reach an understanding of the correlations observed in inclusive reactions.

Figure 6 to illustrate the situation exhibits the values of the $R_{c.c}^{(n)}$ functions in the central and fragmentation regions for the $\pi^- p$ interactions at $p = 40$ GeV/c for $n = 4$ and 10. We see that there are no correlations in the central region,[8)] so the short-range correlations in the central region for the inclusive processes are probably due primarily to the different mechanisms for particle production for various values of n. On the other hand, we have $R_{+-}^{(n)}(|\Delta y| \lesssim 0.2) \sim \ln s$, and this function reaches values of 0.8, 0.4, and 0.3 for $n = 4$, 6, and 8, respectively, at $E_\pi = 360$ GeV (Ref. 49). At the same time we have $R_{--}^{(n)} \approx 0$ at these energies. For low multiplicities there is thus a clustering of the pions

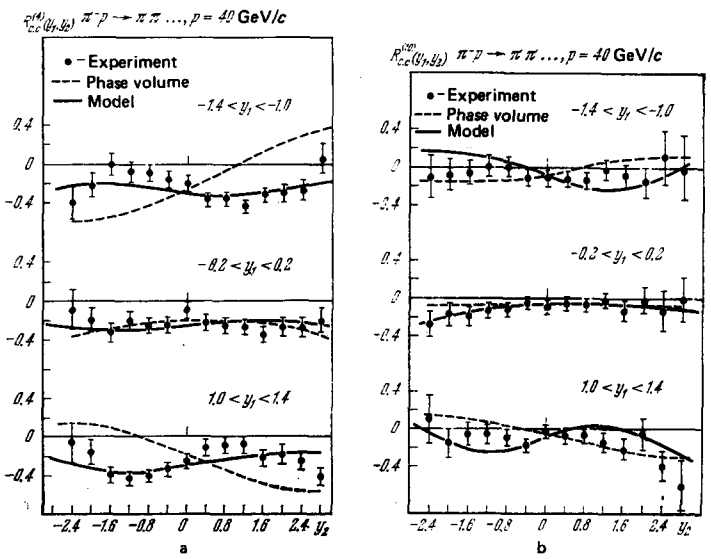

FIG. 6. Values of $R_{c.c}^{(n)}(y_1, y_2)$ for the semi-inclusive reactions $\pi^- p \to n_2 X$ for $p = 40$ GeV/c. a) $n = 4$; b) $n = 10$.

[5)] The value of $\overline{R}_{c.c}(0, 0)$ is given for the interval 40–2000 GeV.

[6)] The integral $\int C_2^{(n)} dy_1 dy_2$ is equal to $-n$ for identical particles or 0 for different pions.

[7)] For $n = 2$, 4, 6, for example, diffractive processes are important; they are unimportant at $n > 6$.

[8)] Small positive correlations [$R^{(n)}(0, 0) \approx 0.1 - 0.2$] are observed in the larger statistical base for $(\pi^+\pi^-)$ pairs.

of different signs, and this effect may be related to the production of resonances (ρ^0, ω^0) or heavier clusters.[49] At high multiplicities, it becomes essentially impossible to distinguish two-particle correlations associated with resonances or clusters because of the large number of "false" combinations. In this case it becomes necessary to study the many-particle correlations among the secondary particles.[50]

b. Azimuthal correlations

The two-particle correlations among the secondary particles can also be analyzed in the plane perpendicular to the momenta of the primary particles. The usual procedure is to examine the distributions of particle pairs with respect to φ, the azimuthal angle between the particles. Here

$$\cos\varphi = (\mathbf{p}_{\perp 1}, \mathbf{p}_{\perp 2})/|\mathbf{p}_{\perp 1}||\mathbf{p}_{\perp 2}|, \qquad (3.15)$$

and the analysis is carried out for various y, Δy and $p_\perp$ ranges. Figure 7 compares the experimental data with the phase-volume and multiperipheral calculations for the $\pi^- p$ interactions at $p = 40$ GeV/c (Ref. 48). For the most part, the theoretical curves give a satisfactory description of the data, but this is not the case for the region $\varphi \to 0$, especially for the $(\pi^- n^-)$ pairs. A special analysis was thus made of the $dN/d\varphi$ distributions for identical pions and different pions.[48,21] It turns out that if the $(\pi^+\pi^-)$ pairs from the vicinity of the ρ^0 resonance $[M(\rho) \pm \Gamma(\rho)]$ are eliminated from consideration the difference in the behavior of the $(\pi^-\pi^-)$ and $(\pi^+\pi^-)$ pairs diminishes at $|\Delta y| \lesssim 1$. This difference remains significant, however, for $|\Delta y| \lesssim 0.4$. The observed effect is thus due both to resonance production and to the identical nature of the pions. This identity of particles makes itself felt particularly distinctly in azimuthal correlations if the difference between the

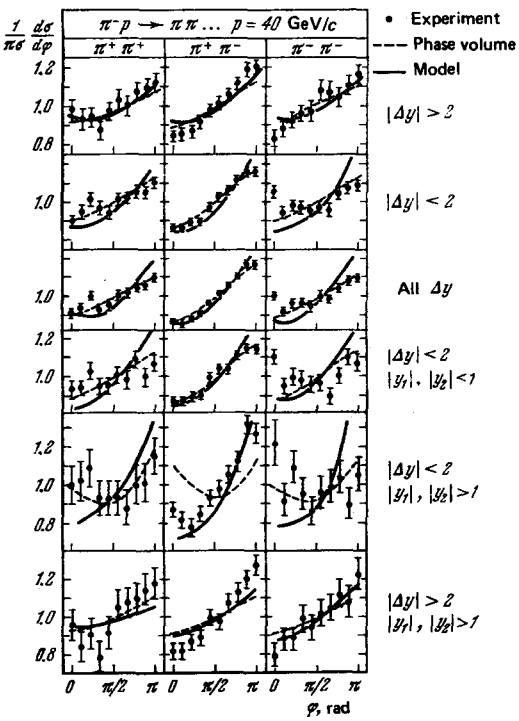

FIG. 7. Azimuthal correlations in $\pi^- p \to \pi\pi X$ processes in various Δy intervals, as specified at the right ($p = 40$ GeV/c).

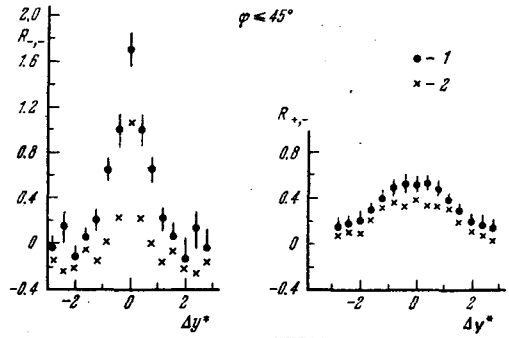

FIG. 8. Inclusive correlations R_{--} and R_{+-} for the reactions $\pi^- p \to \pi\pi X$ at $p = 200$ GeV/c for azimuthal angles $\varphi \leq 45°$. 1) For $p_\perp$, the pion transverse momentum, between 0 and 0.15 GeV/c; 2) $p_\perp = 0.25$–0.50 GeV/c.

momenta of the two particles is very small, $\Delta p_{\perp,2} \to 0$. Figure 8 shows the values of R_{--} and R_{+-} as functions of Δy^* for $\pi^- p$ interactions for $p = 200$ GeV/c and $\varphi \leq 45°$ (Ref. 51). It follows from this figure that in the limits $\Delta p_\perp \to 0$ and $\Delta y \to 0$ there are strong short-range correlations for the $(\pi^-\pi^-)$ pairs $[R_{--}(0) = 1.6(!)$, while $R_{+-}(\Delta y \approx 0) \approx 0.4]$.

In summary, a study of the two-particle correlations among the secondary particles over a broad energy range (10–2000 GeV) resulted in the observation of important short-range correlations. These correlations are due both to the different mechanisms for particle production at different multiplicities and to the formation of clusters or resonances. The azimuthal correlations reveal an effect due to the identical nature of the secondary particles, and this effect will be discussed in Section 5. On the other hand, the standard correlation functions turn out to be relatively insensittive to the clustering of the particles. Two versions of the multiperipheral model with different cluster fractions give satisfactory descriptions of the two-particle correlations over a broad energy range. In order to determine the mechanisms for the particle production at high energies, multidimensional distributions should accordingly be studied, because the statistical base of events must be sharply increased.[50] A slightly different approach was suggested in Refs. 23 and 52, where a study was made of the semi-inclusive distributions with resepct to rapidity intervals including several particles, i.e., the distributions with respect to the quantities

$$\Delta y_{i,k} = y_{i+k+1} - y_i, \qquad (3.16)$$

where i is the index of a particle in the event, assigned according to rapidity, and k is the number of particles within the interval. The distributions with respect to rapidity interval turned out to be sensitive to the role played by the clustering of secondary particles.[23] A study of quantities of the type $\Delta y_{i,k}$ with $k \neq 0$ implies a transition to many-particle correlations, but this transition is extremely difficult to make in the course of an ordinary generalization of the correlation functions $C(R)$ because of the large number of variables. At any rate, further determination of the multidimensional correlations and their analysis pose the complicated problem of finding the necessary variables to reflect the dynamics of the process. It would be impossible to solve this problem without comparing

the various models with experiment through a computer simulation of events.[41-43]

4. PRODUCTION OF RESONANCES

The discovery that large numbers of resonances are produced in high-energy inclusive reactions greatly affected our understanding of the dynamics of multiple-production reactions. Up to about 1976 (up to the Eighteenth International Conference on High-Energy Physics, held in Tbilisi in 1976) it was generally believed that at $E \gtrsim 10$ GeV the particle produced in greatest numbers were the lightest of the hadrons (the pions), and at first glance the experimental data[16-20] seemed to confirm this belief ($\approx 90\%$ π, $\approx 10\%$ K). In this connection it also appeared that there was a strong deviation from $SU(3)$ or $SU(6)$ symmetry in the multiple-production processes, despite the success of these symmetries in the classification of hadrons in unitary multiplets.

As the experimental results accumulated, and as techniques for distinguishing short-lived resonances improved, however, it became clear that these resonances constitute a substantial fraction of the secondary particles.

It thus turned out that what had been studied up to that point had consisted largely of products of the decay of these resonances, and these products of course reflected the dynamics of the strong interactions only weakly. The main tendency in the recent experiments on inclusive reactions has accordingly been to study the production of resonances.

Since this question is very important, we will discuss the method for distinguishing the resonant states at high energies and the reliability of the resulting data (Subsection 4a). Subsection 4b gives data on the production of vector mesons ($\rho, \omega, K^*, \varphi$), the first results on the production of heavy mesons [$f, K^*(1420)$], and the possible fraction of pions which are not products of the decay of short-lived particles ("direct" pions). In Subsection 4c we will discuss the basic features of the momentum spectra of the resonances and their interpretation according to the additive quark model (Subsection 4d). Certain characteristics of resonance production were discussed in Ref. 22, so we will make the discussion here very brief, and we will work primarily from new data.

a) Procedure for distinguishing the resonances

Experimentally, of course, only relatively long-lived particles (π, K, N, Λ, etc.) are detected. None of the short-lived resonances or clusters (ρ^*, K^*, N^*, etc.) are observed directly; only their decay products are observed ($\rho \to 2\pi$, $K^* \to K\pi$, $N^* \to N\pi$, etc.). The measured ratios of the particle yields are thus not the ratios corresponding to the time at which the particles are produced. In order to determine what is produced in hadron collisions, it is necessary to study the production of particles (or clusters) with a short lifetime ($\tau \sim 10^{-23}$ sec):

$$a + b \to R + X. \tag{4.1}$$

This study is based on the products of their decay into pions, kaons, nucleons, etc.

At low energies ($E \lesssim 10$ GeV), the resonances (R) are distinguished using the effective-mass spectra, for example, examining $M(\pi^+\pi^-)$, in which peaks are observed in the mass region corresponding to the ρ^0 meson. In this case we have $\langle n \rangle \approx 3$, and the "signal-to-background" ratio is usually $r \approx 2$–5. There is accordingly no problem in drawing the background curve below the peak corresponding to the resonance. The systematic uncertainties in the background curves, ≈ 10–20%, lead to an error $\lesssim 10\%$ in the determination of $\sigma(R)$. The situation is very different at high energies, at which many particles are produced ($\langle n \rangle = 10$–20). Even in the most favorable case, in which only resonances (e.g., ρ^0 mesons) are produced, their number is $N(\rho) = n/2$, while the number of "false" combinations, i.e., pairs of pions from the decay of various resonances, is $N(\pi^+\pi^-) \sim n^2$, and we have $r \sim 1/n$. In 1970–1974, while the number of events in multiple-production experiments was low ($\lesssim 5000$), the "signal" corresponding to the ρ^0 mesons at $E \gtrsim 20$ GeV was accordingly not detected. Only after an increase in the statistical base to tens of thousands of events was a small "knee" observed in the mass region corresponding to the ρ^0 resonance ($r = 0.05$–0.10). This knee corresponds to a small contribution of ρ^0 mesons ($\approx 20\%$) to the production of secondary pions. This discovery broke the psychological barrier, and the race was on to study the high-energy production of resonances.

The standard method for distinguishing resonant states is still in use. The effective-mass (M) spectra are approximated by an equation of the type

$$\frac{dN}{dM} = \Phi_1(M) + \Phi(\mathrm{BW}(M))\,\Phi_2(M), \tag{4.2}$$

where $\Phi(\mathrm{BW})$ are the Breit-Wigner functions and $\Phi_i(M)$ are the background curves, which are usually written in the form $\exp(\alpha M + \beta M^2)$ or as a polynomial of degree n. Equation (4.2) thus ignores the interference of the resonanc and background states and the "reflection" of the decay of other resonances, which could substantially alter the shape of the background curve.

At low energies ($p_\pi = 7.5$ GeV/c) these "reflection" effects are taken into account in determining the characteristics of the resonances.[53] This was done for high energies ($E_\pi = 40$ GeV/c, $E_p = 1473$ GeV) in Refs. 54–57. As a typical high-energy distribution and to illustrate the "reflecting" effects, we show in Fig. 9 the distribution with respect to $M(\pi^+\pi^-)$ obtained in pp interactions at $E_p = 1473$ GeV (ISR).[57] The arrows show the values of $M(\rho^0)$ and the maximum of the $M(\pi^+\pi^-)$ spectrum resulting from the decay $\omega \to \pi^+\pi^-\pi^0$; the dotted curve is the background curve obtained for $(\pi\pi)$ combinations from various events and normalized in the region $M = 2.04$–4.0 GeV. Figure 10 shows the $M(\pi^+\pi^-)$ spectrum after the background curve has been subtracted. Here we can clearly identify "signals" corresponding to the decay events $\rho^0 \to \pi^+\pi^-$ and $\omega \to \pi^+\pi^-\pi^0$. The huge contributions from the resonance decay are thus masked in the original, nearly smooth curve. To extract these contributions is thus a complicated problem, for which

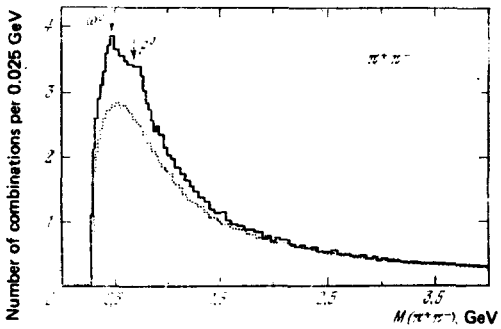

FIG. 9. Effective-mass distribution of $(\pi^+\pi^-)$ pairs in pp interactions at $E_p = 1473$ GeV. The dotted curve is the background (see the text).

the background curve must be chosen correctly. An error of 10–20% in the choice of this background curve would change the resonance-production cross section by a factor of two. From this example we can also clearly see that it is necessary to take into account the "reflection" of the decay events $\omega \to \pi^+\pi^-\pi^0$ in the $M(\pi^+\pi^-)$ spectra in order to determine the characteristics of the ρ^0 production. Both the decays $\eta \to \pi^+\pi^-\pi^0(\gamma)$ and $K^{*0} \to K^\pm\pi^\mp$ are also important, however, the latter for reasons stemming from the particular procedure used: The charged kaons are indistinguishable from $\pi^\pm$ mesons at high energies. Analysis of the $M(\pi^+\pi^-)$ spectrum on the basis of (4.2) taking "reflection" effects into account, which are unambiguously determined by the matrix elements for the decay of the ω and η mesons, leads to the values of $\langle n(R)\rangle$, the average number of resonances per pp interaction[57] (Table II). As an example, Fig. 11 shows the contributions from the decay of the ρ^0, ω, η, K^*, and f mesons to the distribution. The average number $\langle n_{ch}\rangle$ due to the decay of the ρ^{*0}, ω, and $K^{*\pm 0}$ mesons is 10.3 ± 1.2, while direct measurements yield[9] $\langle n_{ch}\rangle = 10.3 \pm 0.1$ (Ref. 27). Jancso *et al.*[57] conclude that the yield of resonances from all the pions and kaons is $(100 \pm 20)\%$ or $\geq 60\%$ at the 95% confidence level. In summary, the results obtained on the Serpukhov accelerator[54-56] ($p_\pi = 40$ GeV/c) and the ISR[57] ($E_p = 1473$ GeV) reveal that the secondary particles are predominantly resonances.

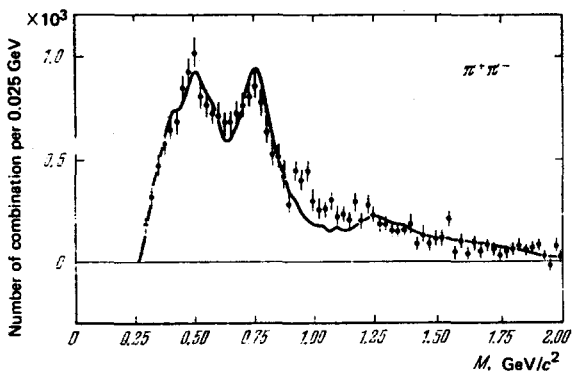

FIG. 10. Distribution with respect to $M(\pi^+\pi^-)$ after substraction of the background ($E_p = 1473$ GeV).

[9]Here it is assumed that $\sigma(\rho^0) = \sigma(\rho^+) = \sigma(\rho^-)$ and $\sigma(K^{*0}) = (K^{*+}) = \sigma(K^{*-}) = \sigma(K^{*0})$.

TABLE II. Average numbers of resonances (pp, $\sqrt{s} = 53$ GeV).

Resonance	$\langle n(R)\rangle$ (all resonance-decay modes)	Resonance	$\langle n(R)\rangle$ (all resonance-decay modes)
ρ^0	1.19 ± 0.25	η	0.92 ± 0.58
ω^0	1.59 ± 0.28	f	0.43 ± 0.24
$K^{*0} + \bar{K}^{*0}$	1.14 ± 0.35		

At the time of this writing, about 50 papers have been published on the inclusive production of resonances in pp, $\pi^\pm p$, $\bar{p}p$, $K^\pm p$, np, and $\pi^- d$ interactions at momenta from 0.7 to 1473 GeV/c.

As a rule, the data for $E \lesssim 20$ GeV have a large statistical base, and the "reflection" effects and "false" combinations ($\langle n_{ch}\rangle \approx 3$–4) are less important here, because the angles and momenta of the secondary particles have been measured more accurately. These results can thus be taken as definitive. At high energies ($E \gtrsim 20$ GeV), "reflection" effects have been neglected in all the papers except Refs. 54–57. Furthermore, the experimental resolution in this energy range is worse than at $E < 20$ GeV, so we should expect refinements in the data for this energy range.

b. Cross sections for resonance production

The most complete information available is that on the high-energy production of ρ^0 mesons:

$$a + b \to \rho^0 + X, \tag{4.3}$$

where

$$\rho^0 \to \pi^+ + \pi^-. \tag{4.4}$$

Figures 12 and 13 show data[25] on $\sigma(\rho^0)$ and $\langle n(\rho^0)\rangle$. Shown for $E = 40$ GeV/c are two values of $\sigma(\rho^0)$ and $\langle n(\rho^0)\rangle$, obtained with (the dashed line in Fig. 13) and without an account of the "reflection" of the $\omega \to \pi^+\pi^-\pi^0$ decay events. An extrapolation of the data from $E \lesssim 200$ GeV to $E = 1473$ GeV yields values smaller than the ISR values with "reflection" of the decay events $\eta \to \pi^+ + \pi^- + \pi^0(\gamma)$ and $\omega \to \pi^+\pi^-\pi^0$ being taken into account.[57] On the other hand, the data[54-56] for $E_\pi = 40$ GeV in which the "reflection" effects have not been taken into account agree well with the results for other energies. In this connection it can be hoped that the behavior as a function of s will not change when the results on $\sigma(\rho^0)$ and $\langle n(p^0)\rangle$ are refined (Subsection 4a).

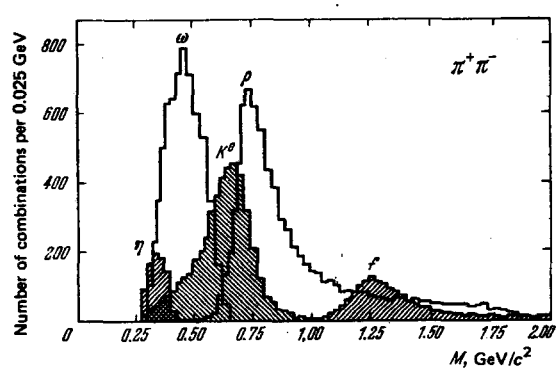

FIG. 11. Contributions of the resonances [η, ω, $K^*(890)$, ρ^0, f] to the $M(\pi^+\pi^-)$ distribtution for pp collisions at $E_p = 1473$ GeV.

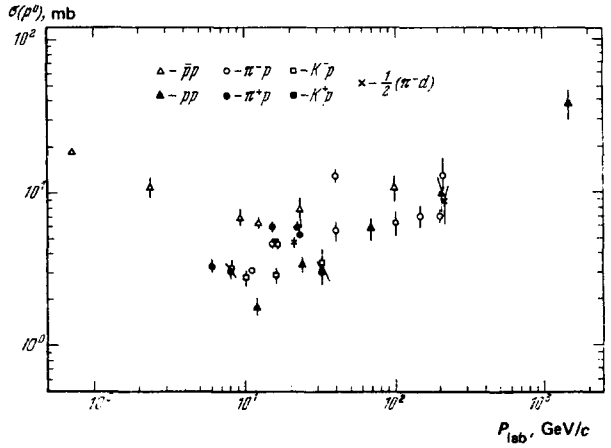

FIG. 12. Variation of $\sigma(p^0)$ with p_{lab} for various reactions.

The differences in the production of ρ^0 mesons in πp and pp collisions are due to the suppression of the fragmentation $p \to \rho^0$. The energy dependence $\langle n(\rho^0)\rangle = f(s)$ for $s = 10$-400 GeV^2 is essentially the same for the two types of collisions[25,26]:

$$\langle n(\rho^0)\rangle^{\pi^+ p} = (0.09 \pm 0.01)\ln s - (0.13 \pm 0.03) \tag{4.5}$$

and

$$\langle n(\rho^0)\rangle^{pp} = (0.09 \pm 0.02)\ln s - (0.23 \pm 0.06). \tag{4.6}$$

We can thus estimate the cross section for the fragmentation $\pi^+ \to \rho^0$ to be

$$\sigma_F(\rho^0) = (0.10 \pm 0.07)\,\sigma_{in}^{\pi p} = 2.0 \pm 1.4 \text{ mb}. \tag{4.7}$$

The differential spectra $\sigma(y)$ are consistent with this conclusion[25,26] (Figs. 14 and 15). It can be seen from the data shown here that in pp collisions at $p = 24$ GeV/c the ρ mesons are produced in the central region and have identical (within experimental error) y distributions. A distribution of this type has been observed for $\sigma^{\rho^-}(y)$ in $\pi^+ p$ interactions at $p = 16$ GeV/c; in other words, the fragmentation $\pi^+ \to \rho^-$ has been suppressed. The fragmentation $\pi^+ \to \rho^{0*}$, on the other hand, is important. Figure 16 shows the normalized cross sections $(1/\sigma_{in})d\sigma(\rho^0)/dy^*$ for $\pi^- p$, $K^- p$, and pp collisions.[25,26] It can also be seen here that the fragmentation $K^- \to \rho^0$ occurs, but to a lesser extent than in the case $\pi^- \to \rho^0$. The data on the cross sections for ρ^0 production thus furnish evidence for the existence of two distinct production regions: a central region and a fragmentation region. Table III shows estimates of the cross sections $\sigma(\rho^0)$ for these two regions for $E = 10$-24 GeV (Refs. 25 and 26). Also shown here are predictions (expressed in relative units) based on the additive quark model (Subsection 4d).

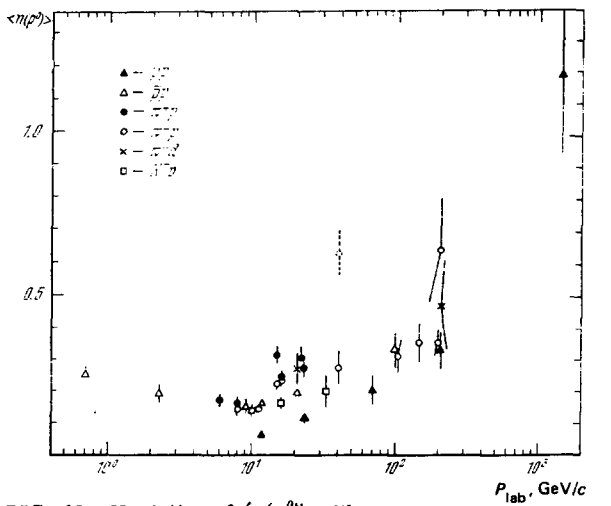

FIG. 13. Variation of $\langle n(p^0)\rangle$ with p_{lab}.

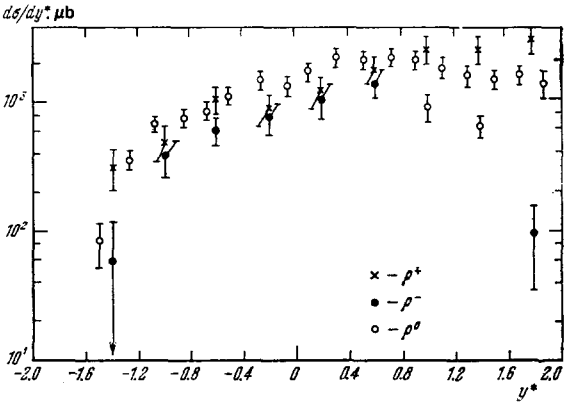

FIG. 14. Rapidity distributions of the ρ^+, ρ^-, ρ^0 mesons in $\pi^+ p$ interactions at $p = 16$ GeV/c.

The most extensive data on the production of other resonances have been obtained for $\pi^+ p$ interactions at $p = 16$ GeV/c (Refs. 25, 26, and 58). These results are listed in Table IV. At $E = 16$ GeV, those meson resonances which have been distinguished themselves furnish 51% of all the observed secondary pions; of these resonances, the vector mesons (ρ, ω) furnish 43%. Analogous results have been obtained in $\pi^- p$ interactions[54-56] and pp interactions[57] at $E_p = 1473$ GeV. It is also interesting to note that while we find $\sigma(K^{*0}(890)) \ll \sigma(\rho^0) \approx \sigma(\omega)$ at $E = 16$ GeV we have $2\sigma[K^{*0}(890)] \approx \sigma(\rho^0) \approx \sigma(\omega^0)$ at $E = 1473$ GeV (Table II). In other words, the $SU(3)$ symmetry may be "restored" at high energies. It would thus seem to be an established fact that at high energies $\gtrsim 60\%$ of the pions are also produced through the decay of vector mesons.[57] Some of the pions are also produced in the decay of baryon resonances, but an effort to distinguish these resonances runs into difficulties in identifying the protons and neutrons. Consequently, we have only pre-

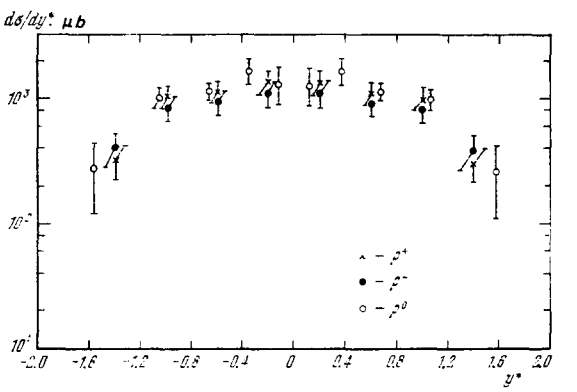

FIG. 15. Invariant cross sections for the production of ρ^+, ρ^-, and ρ^0 mesons in pp collisions at $p = 24$ GeV/c.

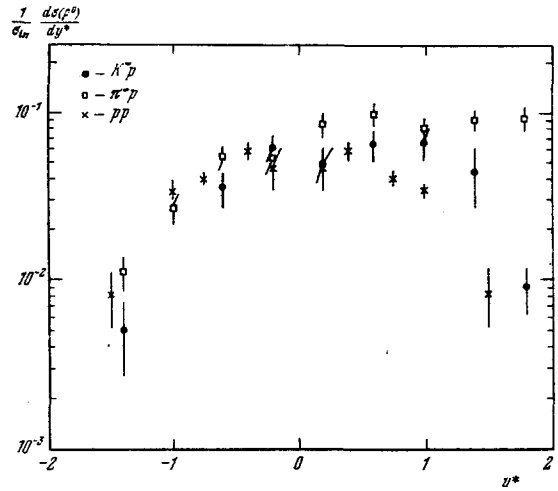

FIG. 16. Distribution of the ρ_0 density as a function of the rapidity for π^-p and K^-p interactions at $p=16$ GeV/c and for pp collisions at $p=24$ GeV/c.

liminary data on $\sigma(\Delta^{++})$ at this point.[22] But where do the other ≈40% of the pions come from? To answer this question we should first estimate the contribution of the heavy resonances [f, $K^*(1430)$, A, B, etc.]. The f/ρ^0 yield ratio is essentially independent of the energy and nature of the primary particles, having the value[25,26] ≈0.2 (Table V).

A similar value has been obtained for the ratios $\langle K^*(1420)\rangle/\langle K^*(890)\rangle$ (Table V). The ratio of tensor mesons ($J^P=2^+$) to vector mesons ($J^P=1^-$) is thus ≈20%, with the implication that these tensor mesons make an important contribution to pion and kaon production. The additive quark model predicts ≳25% for the relative number of mesons which are produced in the decay of P-wave meson states, and this estimate is consistent with the data available on the f, $K^*(1430)$, and g mesons.[59] To experimentally distinguish the heavy resonances (A, B, Q, etc.) is thus the next stage in the study of the dynamics of strong interactions. In summary, about 85% of the observed pions are probably products of the decay of meson resonances.

Another possibility is that the resonances themselves are the products of the decay of heavier resonances or clusters.[23] However, the procedural difficulties in distinguishing them rule out any hope of obtaining such information in the near future (Subsection 4a). New methods for analyzing and distinguishing the resonant states need to be invented if we wish to answer this question. The situation is slightly more hopeful in the case of the $\rho(\omega)$ mesons, which can be detected on the

TABLE III. Production cross sections $\sigma(\rho^0)$ in the central and fragmentation regions ($E=10-24$ GeV).

Reaction	Beam Fragmentation, $\sigma(\rho^0)$, mb	Quark model	Central region, $\sigma(\rho^0)$, mb	Quark model (AQM)
$\pi^-p\to\rho^0X$	3.1±0.3	3	1.6±0.5	2
$K^-p\to\rho^0X$	1.4±0.6	3/2	1.5±0.5	2
$pp\to\rho^0X$			3.5±0.4 *)	3

*) Listed for the pp collisions are the values of the total inclusive cross section, $\sigma(\rho^0)$; in other words, the contribution from the fragmentation $p\to\rho^0$ has not been separated out.

TABLE IV. Resonance-production cross sections in π^+p interactions at $p=16$ GeV/c.

Resonance	$\sigma(R)$, mb	Contribution to $\sigma(\pi^-)$, mb	Resonance	$\sigma(R)$, mb	Contribution to $\sigma(\pi^-)$, mb
ρ^0	4.8±0.4	4.8±0.4	η'	~0.1	~0.07
ρ^-	2.3±0.5	2.3±0.5	φ	~0.1	~0.01
f	0.99±0.10	0.63±0.07	g^0	0.32±0.20	0.03±0.05
ω	4.0±0.7	3.7±0.6	K^{*-} (890)	0.18±0.05	0.12±0.03
η	1.5±0.3	0.44±0.99	K^{*0} (890)	0.71±0.10	0.47±0.07
All $\sigma(R)$: 12.4 ± 0.9 mb = 51 ± 4% $\sigma(\pi^+p\to\pi^-X)$					

basis of the decay $\rho(\omega)\to\mu^+\mu^-(e^+e^-)$. In this case, even at $E=1473$ GeV, we have $\langle n(R)\rangle\approx1$, so that the signal-to-background ratio is[60,61] $r>1$.

In connection with the dominant role of resonances in hadron interactions, we are naturally interested in the relative number of pions which are not products of the decay of these resonances ("direct" pions). This relative number ranges from 20% to 10% in various estimates.[25,26] The quark-model calculations predict[59] ≈6.5%, so that the characteristics which have been obtained for multiple-production processes (Sections 2 and 3) reflect the dynamics of the production and the kinematics of the decay of the resonances. These characteristics are thus much more difficult to interpret. If we wish to understand the dynamics of strong interactions we must first learn to distinguish resonances well.

c. Universal aspects of the momentum spectra of particles and resonances

In this section we will discuss certain aspects of the behavior of the differential cross sections for the production of resonances ("direct" production of strong interactions) and all secondary particles. Experimentally, these cross sections are determined through the use of Eq. (4.2) for fixed values of the longitudinal variables (x, y) or $p_\perp^2$. In this case, the difficulties in distinguishing the resonant states (Section 4a) are only aggravated, especially at $E\gtrsim20$ GeV. We believe, however, that certain characteristic features in the behavior of the differential cross sections, found primarily at $E\lesssim20$ GeV, are preserved without any important changes.

Figures 14–17 show the values of $d\sigma/dy^*$ and $d\sigma/dx_F$ for the ρ and ω mesons. Hence we can draw the following conclusions, which are confirmed also by other experiments.[25,26,58]

1. The ρ spectra in the central region ($|y|\lesssim1$) are

TABLE V. The ratios $\langle f\rangle/\langle\rho^0\rangle$ and $\langle K^*(1420)\rangle/\langle K^*(890)\rangle$.

Reaction	P_{lab}, GeV/c	$\langle f\rangle/\langle\rho^0\rangle$	Reaction	P_{lab}, GeV/c	$\frac{\langle K^*(1430)\rangle}{\langle K^*(890)\rangle}$
$\pi^+p\to RX$	8	0.30±0.07	$K^-p\to RX$	10	0.16±0.05
	15	0.22±0.05		16	0.11±0.03
	16	0.21±0.02			
	23	0.21±0.05			
$\pi^-p\to RX$	16	0.20±0.04	$K^+p\to RX$	5	0.17±0.08
	40	0.18±0.11		8	0.22±0.09
				16	0.27±0.09
$pp\to RX$	1473	0.36±0.19			
$K^-p\to RX$	10–16	0.18±0.20			
$K^+p\to RX$	32	0.27±0.13		32	0.29±0.07

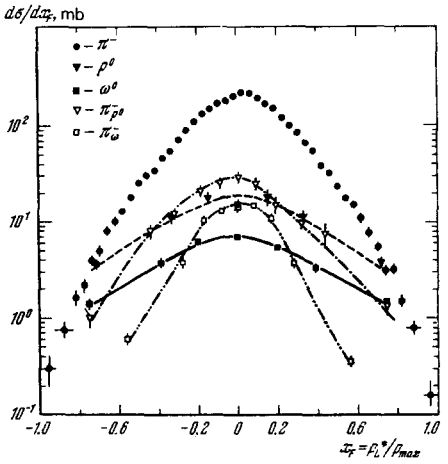

FIG. 17. Distributions of the π^-, ρ^0 and ω^0 mesons and of their decay products (π^-) with respect to x in π^+p interactions at $p = 16$ GeV/c.

independent of the nature of the primary particle, within experimental error. In other words, we have

$$\frac{d\sigma(R)}{dy} = C_i F(y), \tag{4.8}$$

where C_i are the total cross sections for the production of resonances of type i.

2. The spectra of pions from the decay of ρ and ω mesons have a narrower x distribution than do the resonances themselves (Fig. 17). The universal nature of the resonance spectra in (4.8) with respect to the longitudinal variables in the central region shows that these resonances have the same production mechanism. This result was predicted in 1973 on the basis of the additive quark model.[13] The fact that the "decay" pions have a narrower x distribution than that of the resonances may be at least partially responsible for the violation of scaling at $x = 0$ (Section 3).

Some noteworthy features have been discovered in a study of the differential $p_\perp^2$ spectra of the resonances and "direct" pions. These features have been studied in pp, πp, Kp, and $\bar{p}p$ collisions over the momentum range from 0.7 to 240 GeV/c (a table summarizing the results is given in Ref. 58). Data have been obtained for the ρ, ω, η, φ, f, and K^* mesons and for the Δ^{++} and $\Sigma^*(1385)$ baryons. As it turns out, all these cross sections are described well by the equation

$$\frac{d\sigma}{dp_\perp^2} = C_i e^{-Bp_\perp^2} \tag{4.9}$$

with $B \approx 3.4$ (GeV/c)$^{-2}$ over the $p_\perp^2$ range from 0 to 2 (GeV/c)^2 (Fig. 18).[58] The spectra of all the pions have a complicated dependence on $p_\perp^2$, and the reason for this behavior has now been established: most of the pions are produced through resonance decay, so that their behavior at $p_\perp^2 \lesssim 1$ (GeV/c)^2 reflects the kinematics of the decay of various resonances (Fig. 19). Indeed, in the region $p_\perp^2 > 1$ GeV/c, where these decay events make only a small contribution to $d\sigma(\pi)/dp_\perp^2$, they are also described by (4.9) with $B \approx 3.4$ (GeV/c)^2 ("direct" pions). Hence we can estimate the relative number of "direct" pions, by extrapolating the pion data from the region $p_\perp^2 > 1$ (GeV/c)^2 to $p_\perp^2 \to 0$. This relative number

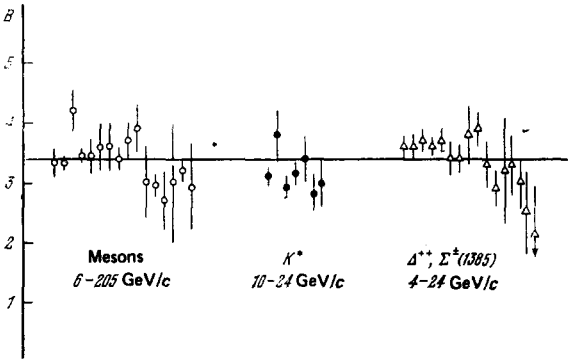

FIG. 18. Dependence of B on mass and energy for particles and resonances.

turns out to be[26,58] ≈10–20%.

A universal aspect has thus been observed in the distribution of the "direct" hadron production for $M = 140$–1400 MeV and $J^P = 0^-, 1^-, 2^+, 3/2^+$; this aspect is characteristic of the statistical models. The $p_\perp^2$ spectra of the heavier particles (J/ψ) are also described by (4.9), but with $B \approx 1.1$ (GeV/c)$^{-2}$ (Ref. 58). At present it is not clear whether this result is due to the variation of B with M or to the nature of the new particles.

Let us examine the results obtained for secondary particles without distinguishing the resonances. Figure 20 shows the values of $\langle p_\perp \rangle = f(M)$ for the system of pions (from two to six) which are produced in pp interactions at $p = 400$ GeV/c (Ref. 58). The dashed line in this figure shows the values of $\langle p_\perp \rangle$ for the $(\mu\mu)$ pairs, while the solid curves are Monte Carlo calculations for the (2π) and (6π) systems. In the region $M \lesssim 2$ GeV, there is essentially no variation of $\langle p_\perp \rangle$ with the pion multiplicity, but there is a strong

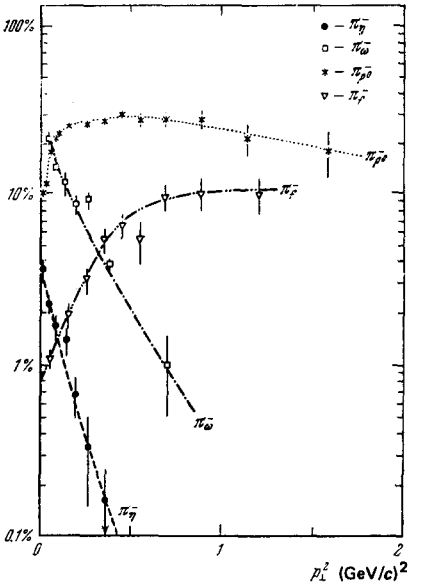

FIG. 19. Contribution of π^- mesons from the decay of η, ω, ρ^0, and f mesons to the inclusive production of π^- mesons as a function of $p_\perp^2$ (π^+p, 16 GeV/c). The curves are sketched in by hand.

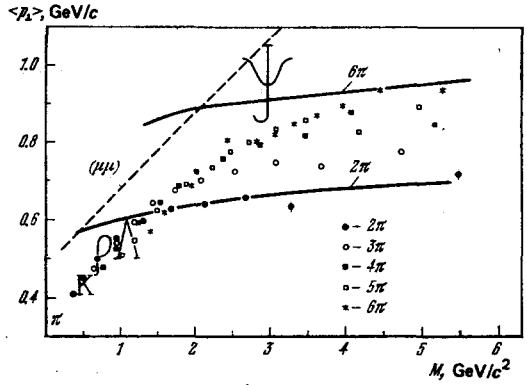

FIG. 20. Variation of $\langle p_\perp \rangle$ with the mass for $(n\pi)$ systems $(n=2-6)$ in pp collisions at $p=400$ GeV/c. Solid curves are Monte Carlo calculations for $n=2$ and 6; dashed line is $\langle p_\perp \rangle$ as a function of $M(\mu^+\mu^-)$.

variation with M. This variation is the same as $\langle p_\perp \rangle = f(M)$ for the π, ρ, N, and Λ particles. In the region $M > 2$ GeV, the variation of $\langle p_\perp \rangle$ with M is weak, but there is a significant variation with the pion number. The values of $\langle p_\perp \rangle$ for the $(\mu\mu)$ pairs and the J/ψ particles are larger than for the pion systems, as in the case of the resonances. These data are consistent with the earlier results, (4.9) ($\langle p_\perp \rangle$ = const), for "direct" hadron production. Indeed, the "decay" pions reduce the values of $\langle p_\perp \rangle$ (Fig. 19) in the region $M \lesssim 2$ GeV; from this follows the dependence $\langle p_\perp \rangle = f(M)$, which was observed already in the late 1950s. At this point we can assume that this variation is due to the kinematics of the resonance decay, rather than to the dynamics of the strong interactions.

Study of the noninvariant differential cross sections for those secondary particles (π, K^0, Λ) and resonances (ρ^0, ω^0) which are produced in the central region $(|y| \lesssim 0.5)$ in π^+p and K^-p interactions at $p=16$ GeV/c shows that these cross sections are described well by

$$\frac{d\sigma}{dE_\perp^3} \sim e^{E_\perp/T}, \tag{4.10}$$

where $E_\perp = p_\perp^2 + M^2$, and T is a parameter which can be interpreted as temperature[10] (Ref. 62). Figure 21 illustrates the situation with the corresponding distributions for the ρ^0, f, and ω mesons ($\pi^+p = 16$ GeV/c). The expression (4.10) satisfactorily approximates not only particles and resonances but also systems of uncorrelated pions[26] $(2\pi, 3\pi, 4\pi)$. Figure 22 shows the values of T found for the particles and resonances for the π^+p and K^-p interactions at $p=16$ GeV/c. Over a broad mass interval (140–1300 MeV), the value of T is 120 MeV (Fig. 22). The $E_\perp - M$ interval from 0 to 1 GeV is roughly the same as the $p_\perp^2$ interval, 0–2 (GeV/c)^2, for which (4.9) holds. At high energies ($\sqrt{s}=31$ GeV) the invariant cross sections $\omega d\sigma/d\mathbf{p}$ are described by $e^{-6E_\perp}$ for π^+, p, and K^+ mesons at $y=0$; this behavior corresponds to $T \approx 167$ MeV (Ref. 64). Taking into account the difference between the

[10] The noninvariant cross sections $d^3\sigma/d\mathbf{p}$ for the production of stable particles are described well by the Planck equation[63]

$$\frac{d\sigma}{d\mathbf{p}} \sim (e^{E_\perp/T} - 1)^{-1}.$$

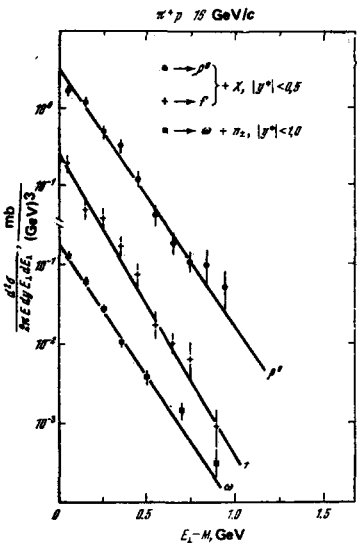

FIG. 21. Cross sections for the production of ρ^0, f and ω mesons as functions of $(E_\perp - M)$ in π^+p interactions at $p=16$ GeV/c. The curves are calculated using Eq. (4.10).

invariant and noninvariant cross sections, we can conclude that the parameter T remains the same from 16 GeV/c up to the ISR energies. This result contradicts the predictions of the statistical model, according to which we would expect[65] $T \sim S^{1/8}$.

A study of the transverse-momentum distributions of multipion systems (from 2π to 6π) in pp interactions at $p=100$ and 400 GeV/c has also shown that, for fixed values of the effective mass, $M=1-3$ GeV, these distributions are essentially independent of three factors: the energy of the primary particles, the charge of the system $(|Q|=0-6)$, and the pion multiplicity.[26]

The invariant cross sections for the secondary particles and resonances at $y \approx 0$ are thus described satisfactorily by (4.10) with $T=120$ MeV over a broad energy range.[11] This behavior is of course consistent with (4.9). A direct conversion from (4.10) to (4.9) leads to a satisfactory description of the $p_\perp^2$ distributions, including the rise of the pion cross sections at $p_\perp^2 \leq 0.5$ (GeV/c)^2. This rise is attributed to the production of these pions as the result of the decay of resonances.[58] The picture of hadron production in

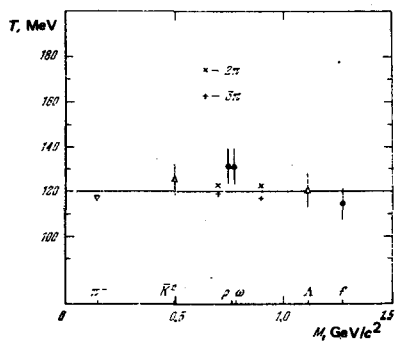

FIG. 22. Values of the parameter T for various particles (K^-p, π^+p, 16 GeV/c).

[11] The invariant cross sections for the pions deviate slightly from exponential, especially at small values of $E_\perp$.

strong interactions which is taking shape is thus surprising. On the one hand, the "direct" hadron production has the universal $p_\perp^2$ distribution (4.9) with $B=3.4$ (GeV/c)$^{-2}$, and the pion distribution is governed primarily by the kinematics of the resonance decay. On the other hand, the pions and resonances in the central region are described by (4.10) with $T \approx m_\pi$, that is, as a state of a thermodynamic system with a constant temperature. At this point it is difficult to say whether this result is simply a coincidence or whether behind it lurks a conversion of the field picture of the hadron interaction into a thermodynamic system.[66] To resolve this question we need new data, especially for the pions and kaons, which differ in mass from resonances. By studying this behavior as a function of the primary-particle energy, especially at $E \gtrsim 1$ TeV, and by distinguishing the "direct" hadron production, we can find the range of applicability of (4.9) and (4.10). However, it is clear already at this point that the characteristics of the secondary particles in the case $y \approx 0$ can also be described, in first approximation, by the statistical model with a constant temperature[67] ($T \approx m_\pi$). Study of the differential cross sections for the production of resonances and particles has thus revealed new aspects of this production and has has explained the growth of $\langle p_\perp \rangle$ with increasing particle mass.

d. Additive quark model (AQM)

Many papers have been devoted to a theoretical interpretation of multiple-production processes.[20,22-24] Pioneering work in this field with cosmic rays led to some simple phenomenological ideas regarding multiple-production processes,[16,17] and statistical-hydrodynamic models were developed in the 1950s to explain these ideas.[17,20,23] As accelerator data became available, however, it was found that at $E \lesssim 2000$ GeV the basic characteristics of many-particle reactions could not be described by these models. At about the same time, multiperipheral models for strong interactions, intimately related to the Regge approach, began to appear.[23] These two directions were combined in the multiperipheral cluster model, according to which clusters of a statistical type are produced at the vertices of a multiperipheral chain.[41-43] This model gives the most nearly complete description of all the data on multiple-production processes (Section 3). A new stage in the evolution of strong-interaction theory resulted from the hypothesis of a quark structure for hadrons.[9] The quark approach permits a common explanation for the weak, electromagnetic, and strong interactions. The quark models have not been developed as thoroughly as the multiperipheral or statistical models, but they could conceivably reveal the nature of interactions among particles. The various quark models differ primarily in the role assigned to the gluons in the production processes; the simplest of them, the additive quark model (AQM), does not explicitly incorporate gluons.[13] Interest in the AQM arose in connection with the discovery of the abundance of resonances, which had been predicted already in 1973. This model successfully describes the basic aspects of multiple-production processes which were discussed in Section 2, and it uses only a few clearcut assumptions regarding the quark structure of strong interactions. Furthermore, the AQM calculations are relatively simple and accessible to the experimentalist, an important consideration for the practical use of this model. As a result, at all the recent conferences on high-energy physics the experimental data have generally been compared with the AQM.[25,26,58] The success of this simple model can of course be explained by arguing that the data available are only a first approximation of the actual picture of strong interactions (Subsections 4a–4c). As new information becomes available, this range of applicability of this model will also become clear, but at the moment the AQM is good enough to describe the experimental data available, and it is a good basis for understanding the basic aspects of multiple-production processes in hadron-hadron and hadron-nucleus interactions[12] (Refs. 68–71). The AQM has been used successfully to describe the relations between the total cross sections,[72] to describe the relation between the slope of the diffraction cone and the form factor,[73] and to explain the asymmetry of the inclusive spectra in meson-baryon interactions.[74] This model has also been developed and used to describe multiple-production processes.[13,68-71]

d1) Impulse approximation. According to the quark model, a hadron is a composite system similar to a light nucleus; a meson consists of two "constituent quarks" ($q\bar{q}$), while a baryon consists of three (qqq). Each constituent quark consists of a set of point particles or "partons:" the valence quark-parton, which carries the quantum numbers, and the "sea," (or "cloud" of quark-antiquark pairs). In the course of the rapid motion of hadrons, the cloud of virtual particles is reorganized into a cloud of parton-quarks.[8] The "dimensions" of these clouds at the present-day accelerator energies are assumed to be much smaller than the distance between quarks in a hadron; in other words, the clouds are spatially separated. Data on the nucleon form factors are in fact in agreement with $R_N^2 \approx 10$ (GeV)$^{-2}$. At the same time, the "dimensions" of the parton clouds $r^2 \sim d' \ln(p/m_N)$, where $\alpha' \approx 0.26$ (GeV)$^{-2}$, correspond to the slope of the Pomeranchuk trajectory. Hence $r^2 \approx 2.0$ (GeV)$^{-2}$ for $E \approx 1$ TeV (Ref. 69). At $E \gtrsim 10^3$ TeV, the parton clouds thus begin to overlap, and with the accelerators which are presently being planned we would expect changes in the multiple-production picture, e.g., the disappearance of fragmentation particles. At the energies of existing accelerators, the constituent quarks are far apart, and their longitudinal momenta are much larger than the "Fermi" momenta of the relative motion. Under these conditions an attempt can be made to describe the hadron interactions by analogy with the collisions of light nuclei on the basis of the impulse approximation. In other words, one could assume that

[12] We will not take up the quark description of the mass spectrum or statistical properties of the hadrons; this material is covered well elsewhere (see, for example, the review in Ref. 68).

the qq interaction occurs in most cases. The corrections for quark rescattering amount ot 10–15% for the ratios of the total cross sections.[72] Their contribution to multiple-production processes is estimated[70,71] to be about 5–10%.

In the AQM the hadrons thus interact with each other by means of slow partons.[8] As a result, the parton clouds "fall apart," and of the point quarks or partons which are formed in this dissipation each begins to be surrounded by its own "sea" and to coalesce with each other and with "spectator" quarks (which have not interacted), forming mesons (qq), baryons (qqq), and antibaryons ($\bar{q}\bar{q}\bar{q}$). The process is shown schematically in Fig. 23. At this point assumptions are made regarding the momenta of the constituent quarks. Specifically, it is assumed that each quark in the primary baryon carries on an average ~1/3 of the total momentum, while each quark in a meson carries $x \sim 1/2$. The x distribution is relatively narrow. In the AQM, assumptions regarding the hadron structure lead immediately to two distinct multiple-production regions: the central and fragmentation regions, both of which are observed experimentally. In the fragmentation regions, the spectator quarks carry off $\approx 2/3$ of the initial momentum of the baryon (or $\approx 1/2$ of the initial momentum of the meson). The quark arriving from the sea in Fig. 23 has a much smaller momentum. The fastest hadron from the central region carries off $\approx 1/3$ of the momentum of a constituent quark, i.e., $\approx 1/9$ of the total momentum of an incident baryon (or $\approx 1/6$ of the total momentum of an incident meson).[13)] Then the baryons in the fragmentation region have $2/3 \lesssim x \lesssim 5/6$ (for primary baryons), while the mesons have $1/2 \lesssim x \lesssim 3/4$ (for primary mesons).[13] The momentum spread of the spectator quarks and of the quarks from the central sea "smears out" this region, but the estimates can still be used as a first approximation. Finally, the hadrons formed in the central region have $x \lesssim 1/3$. If we wish to apply the quark model to multiple-production processes, we must supplement it with a hypothesis regarding the structure of the central sea and the mechanism for hadron production in the fragmentation regions.[13]

At high energies, many quarks and antiquarks are formed differing in charge, strangeness, and spin projection. The quark model has $SU(6)$ symmetry, so that it is natural to suggest that the probabilities for q and $\bar{q}$ production in the central sea are independent

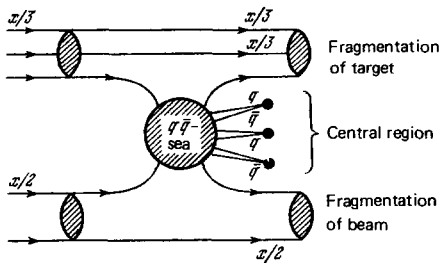

FIG. 23. Hadron-product diagram in the additive quark model.

[13)] This estimate follows from the x distribution of the partons, which is assumed to be homogeneous in ln$x$ (Refs. 13 and 71).

both of their quantum numbers and of the nature of the original colliding quarks.[14)] The strange quarks may represent an exception to this statement, since the number of strange secondary particles is usually smaller than the number of nonstrange particles. For this reason, the parameter λ is introduced; it is a measure of the suppression of the production of strange quarks. For example, in this model we have $\langle n(K^*)\rangle / \langle n(\rho^0)\rangle = \lambda$, which is ≈ 0.20 at $E = 16$–24 GeV (Ref. 58). On the other hand, even at $E = 1473$ GeV the value is[15)] $\lambda \approx 0.5$ (Ref. 57). At the energies available today, it is thus necessary to take into account the suppression of the strange-quark production, but at $E \gtrsim 10$ TeV it may be that all the quarks will be produced in the same manner.

Hadrons are produced through the "coalescence" of quarks and antiquarks. Although the mechanism for this coalescence has not been studied, it is assumed to be independent of the hadron mass.[22] Then hadrons with identical orbital quark states (l) are formed equally probably. This is true, for example, of the baryon 56-plet and the meson 36-plet with zero quark orbital angular momenta. This statement means that the baryon states are represented by an octet of particles with $J^P = 1/2^+$ and a decuplet with $J^P = 3/2^+$, while the mesons are represented by two nonets with $J^P = 0^-$ and $J^P = 1^-$ (Ref. 13). The heavier resonances with $l \neq 0$ have a wave function different from that of the lower $SU(6)$ multiplets, so that the corresponding formation probability may be lower. The experimental values of the ratios $\langle f^0\rangle/\langle \rho^0\rangle$ and $\langle K^*(1430)\rangle/\langle K^*(890)\rangle$ are ≈ 0.2 over a broad energy range.[58,59] It has been found from these data and the AQM that the P-wave mesons states constitute at least 25% of all the mesons which are produced directly in many-particle reactions.[59]

In the AQM model it is also assumed that the probability for the "coalescence" of the spectator quarks with a quark (or antiquark) from the central sea is independent of their quantum numbers. Now that we have introduced these assumptions, we can move on to a description of the particle production in the central and fragmentation regions.

d2) Particle production in the central region ($x \leqslant 1/3$). At high energies at which many quarks are produced in the central sea (Fig. 23), the quarks "forget where they came from," so their momentum distributions are independent of the nature of the primary particles. Since the mechanism for the hadron production from quarks is the same, we can write

$$\frac{d\sigma}{dx\, dp_\perp^2} = C_i F(x,\ p_\perp^2), \tag{4.11}$$

where C_i are the total cross sections for the production of hadrons of type i. The experimental data are de-

[14)] In this regard, this model is the same as the model in which the hadrons in the central region are produced through collisions of gluon clouds (see, for example, the review in Ref. 75).

[15)] Furthermore, the decrease in the number of strange particles may be due to the production of "heavy" resonances, rather than to a breaking of $SU(6)$ symmetry.[59]

scribed well by Eq. (4.11) (Subsection 4c). If it is assumed that there are statistically equal probabilities for all possible combinations of q and $\bar{q}$, it can be shown that the probability for the production of a baryon (qqq) or antibaryon ($\bar{q}\bar{q}\bar{q}$) is one-sixth the probability for the production of a meson ($q\bar{q}$) (Ref. 13.):

$$\frac{\langle n(M)\rangle}{\langle n(B)\rangle} = 6. \tag{4.12}$$

In calculating the relative multiplicity we must take into account the factor $(2J+1)$, which is the number of different spin states. This consideration leads to one prediction of the AQM: that the probability for the production of vector mesons is high in comparison with that for pseudoscalar mesons. This circumstance has in fact been observed recently (Subsection 4b; see also Ref. 13). The ratio of $\langle n(\rho^0)\rangle$ and $\langle n(\omega)\rangle$, which is unity according to the AQM,[16] has also been verified well. This model predicts a relatively large number of antibaryons; in particular, the number of antiprotons should be no lower than one-tenth the number of π^- mesons.[17] At the energies attainable in the Serpukhov accelerator, this ratio is 2–3% at $x \approx 0.14$–0.2 and increases to about twice this value at $E \approx 1000$ GeV. It can thus be concluded that this ratio increases and that an asymptotic value ≈ 0.1 is not improbable. At finite energies, the number of quarks in the central sea is limited, but estimates of the antiproton yield at these energies incorporating this limitation give a satisfactory description of the experimental data.[70]

d3) Fragmentation processes. In the fragmentation region, hadron production is linked to the quantum numbers of the primary particles. The relative probabilities for the hadron yield are easily found by a combinatorial quark calculation.[13] We will explain the situation for the case of meson fragmentation (Fig. 23). The spectator quark (q_i) can capture an antiquark ($\bar{q}$) or a quark (q) from the sea with equal probabilities (1/2). In the case of the antiquark, a fragmentation meson $M_i = q_i\bar{q}$ with $x \sim 1/2$ is produced, while in the quark case $(q/2)+(\bar{q}/2)$ must also be added to the (q_iq) system. Here there is a probability of 1/4 for the appearance of the baryon $B_i = q_iqq$, and there is also a probability of 1/4 for the appearance of a meson, of the sea $M = q\bar{q}$, plus a quark q_i. If q_i is assumed to retain its momentum, then

$$q_i \to \frac{1}{2} M_i + \frac{1}{4} B_i + \frac{1}{4} q_i$$

or, when the following iterations are taken into account,

$$q_i \to \frac{2}{3} M_i + \frac{1}{3} B_i. \tag{4.13}$$

The specific relations for the production of the various types of hadrons have been derived in Refs. 13, 59, and 68–71. Since the hadron-production mechanism is the same in this model, the hadron distributions will be described by the same function. For example, for the fragmentation of protons into baryons we can write

$$\frac{d\sigma}{dx\,dt} = C_{pB}^{(2/3)} F_{pB}^{(2/3)}(x, t). \tag{4.14}$$

Here the superscript (2/3) shows that we are dealing with the fragmentation process $p \to B$ with $x \sim 2/3$ (Fig. 23). The calculations for meson fragmentation are analogous.[13,68-71] The AQM predictions are compared with experiment in Table III. It can be seen from this table that the experimental data agree with the theory within the large errors.

d4) Hadron-nucleus interactions. The quark model in the impulse approximation agree well with experimental data on hadron-hadron interactions. Processes involving the direct interaction of more than one pair of quarks are improbable. The situation is completely different in collisions of hadrons with nuclei.[18] The mean free path of a constituent quark is

$$\bar{l} = \rho\sigma(qN), \tag{4.15}$$

and with

$$\sigma(qN) \approx \frac{1}{3}\sigma_{\text{in}}(NN) \approx \frac{1}{2}\sigma_{\text{in}}(\pi N) \approx 10 \text{ mb} \tag{4.16}$$

this mean free path is 4–5 F (ρ is the density of nucleons in the nucleus). In other words, it is comparable to the radii of intermediate and heavy nuclei. With increasing atomic number of the target nucleus (A), the number of interacting quarks increases, and we have a unique possibility for using nuclei to study the quark structure of hadrons. To calculate the cross sections for the interaction of one, two, and three quarks with a nucleus (Fig. 24) we use the ordinary optical concepts of the passage of a particle through a nucleus of density $\rho(b)$, where b is the impact parameter.[71] In this case the cross sections for these processes for protons ($3q$) take the simple form

$$\sigma_1^P(A) = 3\int d^2b e^{-2\sigma_q T(b)}[1 - e^{-\sigma_q T(b)}], \tag{4.17}$$

$$\sigma_2^P(A) = 3\int d^2b e^{-\sigma_q T(b)}[1 - e^{-\sigma_q T(b)}]^2, \tag{4.18}$$

$$\sigma_3^P(A) = \int d^2b [1 - e^{-\sigma_q T(b)}]^3, \tag{4.19}$$

where $T(b) = A\int \rho(b, z)dz$ is the density of nucleons in the path of the quark, $e^{-\sigma_q T(b)}$ is the probability (W) for the quark to pass through the nucleus without an interaction, and $(1 - W)$ is the interaction probability.[19] The sum of the cross sections σ_1^P, σ_2^P, and σ_3^P is

$$\sigma_{\text{prod}}^{PA}(A) = \int d^2b [1 - e^{-3\sigma_q T(b)}] \approx \int d^2b [1 - e^{-\sigma_{\text{in}}^{NNT}(b)}], \tag{4.20}$$

and it represents the total cross section for the in-

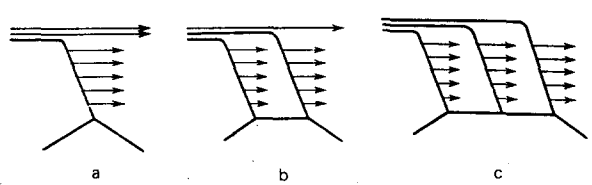

FIG. 24. Inelastic nucleon-nucleus interactions in the quark model. a) A single quark is involved in the interaction; b) two quarks; c) all three quarks.

[16] In this connection the AQM differs from the standard multiperipheral model, with $\langle n(\omega)\rangle < \langle n(\rho^0)\rangle$, because the cross sections for $\pi\pi \to \omega\pi$ or $\rho\pi \to \omega$ are small.

[17] The ratio in (4.12) is higher because of resonance production.[13]

[18] See Refs. 71 and 68 for a detailed bibliography on hadron–nucleus interactions.

[19] Equations (4.17) and (4.19) hold for mesons ($q\bar{q}$) when the substitutions $3 \to 2$, $2 \to 1$, and $3 \to 2$, respectively, are made.

elastic interaction of hadrons with nuclei in the production of at least one secondary hadron, i.e.,

$$\sigma_{prod}^{pA}(A) = \sigma_{in}^{pA} - \sigma_{diss}^{pA}, \tag{4.21}$$

where σ_{diss}^{pA} is the cross section for incoherent quasi-elastic scattering resulting in disintegration of the nucleus. This cross section has not yet been analyzed on the basis of the AQM. The profile functions $T(b)$ are expressed in terms of the known functions $\rho(b, z)$ found from data on the electromagnetic interactions of electrons with nuclei. As a result, the characteristics of the multiple-production processes in collisions with hadrons with nuclei can be predicted on the basis of the quark model and data on hadron-hadron interactions [$\sigma(qN) \approx 10$mb].

Figure 25 shows the relative probabilities for the interaction of one, two, and three quarks with nuclei as functions of A, according to Eqs. (4.17)–(4.20) ($V_i = \sigma_{in}^{hA}/\sigma_{prod}^{hA}$). These results immediately yield several important predictions regarding hadron-nucleus interactions. Obviously, as A increases, the ratio of the multiplicities in πA and pA collisions in the central region should approach 2/3 (according to the number of constituent quarks in the pion and the proton[20]). At the same time, there should be a decrease in the multiplicity of the fragmentation particles with increasing A, because of the decrease in the number of spectator quarks.[71] For the general case it is convenient to express the secondary-particle multiplicities in terms of the multiplicity of qA collisions (n_{qA}):

$$R\left(\frac{pA}{qA}\right) = \frac{n_{pA}}{n_{qA}} = \sum_{k=1}^{3} kV_k^p = \frac{3}{\sigma_{prod}^{pA}} \int d^2b\,[1 - e^{-\sigma_q T(b)}], \tag{4.22}$$

$$R\left(\frac{\pi A}{qA}\right) = \frac{n_{\pi A}}{n_{qA}} = \sum_{k=1}^{2} kV_k^\pi = \frac{2}{\sigma_{prod}^{\pi A}} \int d^2b\,[1 - e^{-\sigma_q T(b)}], \tag{4.23}$$

where

$$n_{hA}(y) = \frac{1}{\sigma_{prod}^{hA}} \frac{d\sigma(hA)}{dy} \tag{4.24}$$

is the multiplicity of the particles in the central region in the collision of particle n with a nucleus. The R_i are thus governed only by the density of nucleons in the nucleus and the qN cross sections. From (4.22) and (4.23) we find that for any nucleus the ratio of the multiplicities in πA and pA collisions is

$$R\left(\frac{\pi A}{pA}\right) = \frac{n_{\pi A}}{n_{pA}} = \frac{2}{3} \frac{\sigma_{prod}^{pA}}{\sigma_{prod}^{\pi A}}, \tag{4.25}$$

which is independent of $\sigma(qN)$. The data available on the πA and pA collisions for the nuclei Ag, Br, Pb, and ^{12}C yield $R \sim 0.8$ in the region $\eta = 1 - 4$ ($\eta = -\ln\tan(\vartheta/2)$, in agreement with the value expected on the basis of (4.25) (Fig. 26; see also Ref. 71).

In the proton fragmentation region with $x \approx 2/3$, hadrons are produced through the attachment of one quark from the sea to two spectator quarks. In the case of pA collisions, the hadrons with $x \approx 2/3$ are thus produced only in the absorption of one of the constituent quarks of the incident proton (Fig. 25a). It follows that

$$R_{p\to B}\left(x \sim \frac{2}{3}\right) = \frac{(1/\sigma_{prod}^{pA})\, d^3\sigma(pA \to Bx)/d^3P}{(1/\sigma_{in}^{pp})\, d^3\sigma(pp \to Bx)/d^3P} = V_1^p(A), \tag{4.26}$$

where $B = p$, n, Δ, Λ, etc.

Equation (4.26) is based on two assumptions; the nucleon consists of three spatially separated quarks, and the process by which the secondary baryon is produced occurs outside the nucleus. At low energies, Eq. (4.26) thus breaks down, since if the third quark is produced inside the nucleus it is absorbed, but this absorption is not taken into account[21] in the equation for $V_1^p(A)$, (4.17). Figure 27 shows the relative yields of the secondary protons in pA interactions for $p_0 = 19.2$ GeV/c and $\theta = 12.5$ mrad, as functions of x and A. The solid curves are the results calculated from the model in which a secondary proton is produced outside the nucleus, while the dashed curve corresponds to production inside the nucleus. The experimental results agree well with the theoretical curves found under the assumption that the secondary protons ($p = 10$–16 GeV/c) are produced outside the nucleus.[71]

In the case of a primary pion, fragmentation mesons or baryons which contain one of the constituent quarks of the incident pion are produced in processes of the

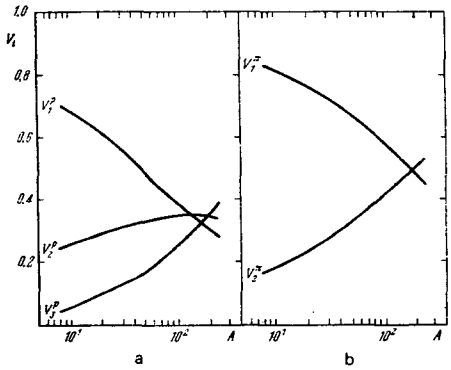

FIG. 25. Relative probabilities for the interaction of one, two, and three quarks as functions of A in pA collisions (a) and πA interactions (b).

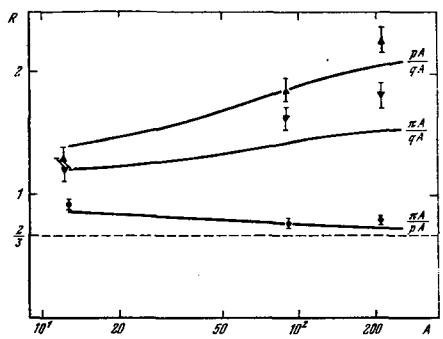

FIG. 26. Values of $R(\pi A/pA)$ as a function of A. The curves are calculated from the model.

[20] As in the case of hadron collisions, the central region is determined by $x \lesssim 1/9$ (for baryons) and $x \lesssim 1/6$ (for mesons).

[21] Hadron absorption inside the nucleus in discussed in Ref. 71.

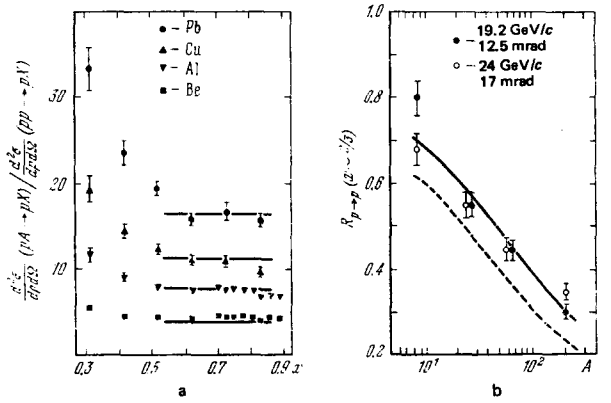

FIG. 27. Secondary-proton yields in pA interactions for $p_0 = 19.2$ GeV/c and $\theta = 12.5$ mrad. a) As a function of x; b) as a function of A. The solid curves and the dashed curve correspond to models in which the secondary proton is produced outside and inside the nucleus, respectively.

type in Fig. 24a, and they have the value $x \sim 1/2$. The ratio of the multiplicities of these particles (h) in the cases of a nucleus and of hydrogen is[71]

$$R_{\pi \to h}\left(x \sim \frac{1}{2}\right) = V_1^{\pi}(A), \tag{4.27}$$

and it is independent of the nature of the fragmentation particle which is produced. Table VI compares the prediction with experiment.[71] In first approximation, the model agrees with the experimental data. Comparing the experimental data with the quark-model calculations, we see that the secondary protons with $p \geq 10$ GeV/c and the secondary π^- and K^+ mesons with $p \geq 6$ GeV/c are produced outside the nucleus[22)] (Ref. 71). Since the radius of the Pb nucleus is about 7 F, it can be assumed that the distance traversed by the particles before the hadron production is at least 4–5 F. In this case we can estimate the constant μ^2, which determines the hadron-production time[71]:

$$c\tau \sim \frac{p}{\mu^2}\hbar c \gtrsim 4 \cdot 10^{-13} \text{ cm}. \tag{4.28}$$

We thus find $\mu^2 \lesssim 0.25 - 0.3$ GeV^2.

Various estimates of this value which have been found from the experimental data through the use of the quark model are discussed in detail in Ref. 71. To conclude this subsection, we give the ratio of the yields of the secondary π^- mesons for the $\pi^-(\nu p)$ and $\pi^- p$ interactions at $p = 40$ GeV/c as a function of the longitudinal momentum in the laboratory coordinate system (Fig. 28). Here ν is the number of protons of the carbon nucleus which take part in the inelastic interactions.[75] In this figure we can clearly see the $\pi^- \to \pi^-$ fragmentation region ($x \gtrsim 1/6$) and the central region ($x \lesssim 1/6$), within which the number of pions is roughly twice that in $\pi^- p$ collisions.[23)] The nuclear fragmentation region ($x \lesssim 0$) has an even more pronounced increase in the π^- multiplicity, possibly because of an increase in the phase volume due to the Fermi motion of the nuclear nucleons.

TABLE VI. Secondary-pion yields in the fragmentation region.

Reaction	p, GeV/c	Variable	R (expt)	R (Theor)
$\pi^- \to \pi^-$ (emulsion)	200	$\eta = 6-7$	0.7 ± 0.1	0.6
$\pi^- \xrightarrow{^{12}C} \pi^-$	40	$x \sim 1/2$	0.85 ± 0.1	0.8 [76]
$\pi^- \xrightarrow{^{12}C} \pi^+$	40	$x \sim 1/2$	0.9 ± 0.15	0.8 [76]

[22)] The AQM calculations may ignore the absorption of fast secondary hadrons inside the nucleus at $p \geq 6$ GeV/c.

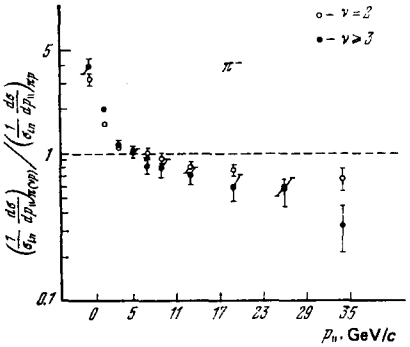

FIG. 28. Ratio of the π^- yield in $\pi^-(\nu p)$ collisions to that in $\pi^- p$ interactions as a function of $p_{\parallel}$ in the laboratory coordinate system. ($p_0 = 40$ GeV/c).

The quark model thus successfully describes the available data on hadron-nucleus interactions. On the other hand, these interactions furnish a unique opportunity for testing the foundations of the AQM, by studying the interactions of one, two, and three quarks with nuclei. According to the same model, we find an estimate of the effective mass (μ) corresponding to the hadron-production time ($\mu^2 \lesssim 0.25 - 0.3$ GeV^2); this is a very important prediction for any strong-interaction model.[8] However, the experimental information available on hadron-nucleus interactions is much less than that available on hadron collisions. The paucity of information is due primarily to the complexity of the theoretical interpretation of this information. The extension of the quark model to interactions with nuclei will undoubtedly stimulate new experiments in this field of high-energy physics.

d5) Discussion of results. The additive quark model gives a satisfactory description of the basic features of multiple-production processes at high energies: the relation $\langle n \rangle = f(s)$, KNO scaling, the relative multiplicities of the secondary hadrons, their energy dependence, multiplicity correlations, etc.[13,59,68-71] The basic predictions of this model, however, have been due to the two-step (or multistep) nature of the production of secondary pions and kaons. The relative number of "direct" pions is small according to the AQM, having the value[59] ≈6.5%. As a rule, the products of the decay of resonances have momenta which are far different from the momenta of the resonances themselves.[24)] Their distributions are accordingly very different from (4.11) and (4.14). For

[23)] Values $\nu \geq 2$ mean that both constituent quarks of the pion participate in the interactions.

[24)] This point is not as important for hadron–nucleus interactions, since these interactions are usually compared with hadron collisions.

example, in the decay[13] $\Delta \to N + \pi$, we have

$$0 \leqslant \frac{x_\pi}{x_\Delta} \leqslant 1 - \left(\frac{m_N}{m_\Delta}\right)^2 \tag{4.29}$$

and

$$\left(\frac{m_N}{m_\Delta}\right)^2 \leqslant \frac{x_N}{x_\Delta} \leqslant 1, \tag{4.30}$$

if $p_\perp(\Delta) \approx 0$ and $x_\Delta \lesssim 1$. Even the fastest pions thus have $x_\pi \approx 0.4 x_\Delta$.

In the decay $\rho \to 2\pi$ we have

$$0 \leqslant \frac{x_\pi}{x_\rho} \leqslant 1. \tag{4.31}$$

As a result, at the energies available, for which $\langle n_{ch} \rangle$ is relatively small, the pions and the kaons from the decay of resonances with $x > 1/2$ make an appreciable contribution to the central region and substantially change the distributions of the type (4.11). Consequently, the real test of the AQM began in 1976, after the experimental identification of short-lived particles. The basic aspects of the resonance production which are described in Subsections 4b and 4c agree satisfactorily with the AQM predictions made already in 1973 (Ref. 13). The next step is to study the production of heavy resonances, which constitute at least 25% of all the mesons which are produced directly in hadron interactions, according to the AQM.[59] It is also necessary to study the production of baryon resonances, especially in the fragmentation regions. New possibilities for studying both the structure of hadrons and the space-time pattern of the strong interactions are presented by the hadron-nucleus interactions. The quark models are particularly attractive because they promise a common description of the weak, electromagnetic, and strong interactions at high energies.[8,75] In this connection, we have already seen some progress in the description of "hard" collisions, in which distances small in comparison with the hadron dimensions play an important role.[77,78] There is accordingly definite interest in the possibility of a quark description of the "soft" processes, which constitute ≈80% of the total cross section for hadron interactions.

The model discussed above is the first step toward a dynamic description of multiple-production processes. For the most part, it is based on nothing more than rough estimates of the momenta of the constituent quarks, which is what made it possible to analyze hadron production in the central and fragmentation regions. Its most important predictions deal with the symmetry properties of the strong interactions of quarks, e.g., the relative multiplicities of the particles of the various species in various types of interactions (hh, hA). To establish these properties is itself one of the basic goals of physics. On the other hand, the questions related to the dependence of the cross sections on the momentum components of the detected particle, to the behavior of the total multiplicity, to the energy increase, etc., are also basic in the theory of strong interactions. Of primary importance here is an experimental study of the resonance and pion distributions in the central region [see (4.9) and (4.10)]. Is a thermodynamic description a random combination of the production and decay characteristics of resonances in the given energy range, 10–24 GeV, or is this the nature of quark interactions? Analysis of the quark structure of strong interactions leads to an explanation for the existence of leading (fragmentation) particles, which carry off most of the momentum of the primary hadrons (≈1/2–1/3); this question of course caused difficulty in the statistical-hydronamic models[25] (Refs. 18–20 and 75). A further generalization of the quark models would involve the use of common distribution functions for the quarks and gluons in the nucleons, and these distribution functions are usually taken from experiments on deep inelastic lepton scattering.[8,20,22,23,75] Here we have a case in which we do not have enough experimental information (Subsections 4b–4d), while we are blessed with a multitude of theoretical models, each of which can explain certain features of the experimental data. In this review we accordingly discuss only the "symmetry" features of the quark model and its predictions in two regions of phase space (the central and fragmentation regions). To extend this model we would need much more experimental data on both strong and electromagnetic interactions of the particles, especially at high energies ($E \gtrsim 100$ GeV).

5. INTERFERENCE OF IDENTICAL PARTICLES AND DIMENSIONS OF THE REGION FROM WHICH THEY ARE EMITTED

The difficulty in interpreting many-particle reactions at high energies makes it particularly valuable to have analysis methods which are based on the general principles of quantum mechanics. Among these methods are those based on a study of the interference of identical particles in inclusive processes,

$$a + b \to c\,(p_1) + c\,(p_2) + X, \tag{5.1}$$

from which we can learn about the spatial and temporal "dimensions" of the region from which the secondary particles are emitted. These characteristics are quite different in the different versions of the statistical-hydrodynamic approach. For example, in the statistical model with an expanding volume, the emission region is a sphere of radius $R \sim (\sqrt{s})^{1/3}$, in the hydrodynamic theory for slow particles it is a sphere of radius $R \sim 1/m_\pi$, and in the Fermi theory it is an ellipsoid with[20] $R_\perp \sim 1/m_\pi$ and $R_\parallel \sim M_N/m_\pi\sqrt{s}$. In the multiperipheral models these correlations are related both to the characteristic distances between the vertices of one "comb" and to the correlations of hadrons from different "combs." In the parton models the region in which the hadrons are produced in determined by the parton momentum [see (4.28)], so that this region is different for slow and fast particles. On the other hand, the hadron distributions in the central region are apparently statistical in nature (Subsection 4c). Furthermore, the dimensions of the region of pion and kaon emission are also determined by the resonance lifetimes in all cases (Subsection 4b). This abundance of possibilities for the shape of the hadron-

[25] The peripheral nature of the collisions and the appearance of leading particles are the basis of the multiperipheral models.[20,23]

production region in the various models means that an experimental study at this point is necessary.

Turning to the field of optics, we note that it was established a long time ago that there are angular correlations between the photons emitted by two independent excited atoms. The probability of detecting two-photon events is improved if θ, the angle between the photon momenta, the wavelength λ, and R, the distance between the radiators satisfy

$$\vartheta \leqslant \frac{\lambda}{R}. \tag{5.2}$$

In this sense the emission from the independent sources is coherent. Condition (5.2) is the basis for the Hanbury Brown-Twiss method for measuring stellar diameters.[79]

At high energies, at which many particles are produced, an analogous method can be used for multiple-production processes. As it turned out, the duration of the production process could also be determined by supplementing the angular correlations with energy correlations. In contrast with the standard approach, the emphasis here is on the spatial-temporal characteristics of the production process, rather than the momentum-energy characteristics.

The possibility of using the correlation method for measuring the dimensions of sources was first demonstrated in connection with the so called GGLP effect, in which an excess of pairs of identical pions with relatively small emission angles was observed.[80] This effect was discovered in $\bar{p}p$ annihilation and explained by the statistical theory as a consequence of the Bose symmetrization of the pion wave function. This effect has subsequently been repeatedly studied in a variety of interactions at various energies. The situation has proved very complicated and confused.

The modern correlation method is the result of work over the past six years.[81-86] The picture is much clearer as a result. Here we have in mind the symmetrization of the amplitude for observing, for example, two identical pions which are emitted at different times and from different parts of the emission volume. As a result, there are interference correlations, which raise the probability for detecting identical pions with approximately equal momenta.

The corresponding equations are model-dependent but have the same structure. For example, if the sources are "switched on" simultaneously, if they lie on a sphere of radius R, and if their lifetime is τ, then the probability for observing pions with momenta ρ_1 and ρ_2 is[82-85]

$$W = W_0 (1 + \Delta),$$

where

$$\Delta = \frac{[2J_1(q_\perp R)/q_\perp R]^2}{1+(q_0\tau)^2} \approx \frac{\exp[-(1/4)q_\perp^2 R^2]}{1+(q_0\tau)^2}. \tag{5.3}$$

Here $q_0 = E_1 - E_2$, $\mathbf{q} = \mathbf{p}_1 - \mathbf{p}_2$, $q_\perp$ is the projection of $\mathbf{q}$ onto the plane which is perpendicular to $\mathbf{P} = (\mathbf{p}_1 + \mathbf{p}_2)/2$, and $J_1(q_\perp R)$ is the Bessel function of order one. The coefficient W_0 corresponds to the background distribution (without interference). It is usually determined by using $\pi^+\pi^-$ pairs, although even in this case there could be an interference, in principle.[81-85] Combinations of pions from different events are also used as the background.

The parameters R and τ can be determined from observing $(\pi^\pm\pi^\pm)$ pair correlations and using Eq. (5.3). In general, the quantity τ has a complicated physical meaning.[84] It consists of the average lifetime of the sources (τ_1), the spread in the times at which the sources are switched on (τ_2), and the "longitudinal time" $\tau_3 = R/v$, where v is the pion velocity. The quantity R is related to the distance between the sources which emit identical pions with approximately equal momenta. In the statistical models this quantity is the same as the total dimension of the emission region, while in the multiperipheral models R is probably a measure of the distance between adjacent vertices of the diagram. If the pions are produced in the decay of long-lived resonances rather than immediately, then R and τ are determined by the mean free path and lifetime of these resonances.[87]

The correlation method yields information on the spatial-temporal characteristics of the particle-emission region, and this is important information for a study of the dynamics of strong interactions.

Experimental results have been obtained for $\pi^\pm p$, $K^\pm p$, $\bar{p}N$, pp, and pion-carbon interactions over the momentum range 0–1400 GeV/c (Refs. 25, 26, and 88–91). The values of R and τ have been determined by comparing with equations of the type of (5.3) both the two-dimensional distributions with respect to q_1^2 and q_0 and the one-dimensional distributions with respect to q_1^2 or q_0, with restrictions on q_0 or q_1^2, respectively. Figure 29 illustrates the situation with a plot of the ratio $N(\pi^\pm\pi^\pm)/N(\pi^+\pi^-)$ against q_1^2 for $q_0 \leqslant 0.2$ GeV for K^-p interactions at $p = 16$ GeV/c. The curve is the result of an approximation on the basis of Eq. (5.3) for $q_0 \leqslant 0.2$ GeV/c with $R \approx 1.8 \cdot 10^{-13}$ cm (the statistical base is 70 000 events!). Table VII shows the values of R and τ found experimentally.[25,26,88-90]

It follows from these results that the effect exists

TABLE VII. Dimensions of the region from which the secondary pions are emitted.

Reaction	Momentum, GeV/c	R, 10^{-13} cm	$c\tau$, 10^{-13} cm
1. $\bar{p}n \to 3\pi^-2\pi^+n$	1.0—1.6	1.29 ± 0.06	1.47 ± 0.16
2. $K^+p \to K^+p2\pi^+2\pi^-$	8.25	0.80 ± 0.08	~ 1.0
3. $pp \to pp\pi\pi X$ $(n_\pm \geqslant 6)$	28.5	$R_\parallel = 0.73\pm0.11$ $R_\perp = 1.65^{+3.6}_{-1.0}$	0.6 ± 0.2
4. $\pi^-p \to \pi\pi X$ $(n_\pm \geqslant 6)$	40	$R_\parallel = 1.1\pm0.4$ $R_\perp = 2.3\pm0.5$	0.7 ± 0.5
5. $\pi^-C \to \pi\pi X$ $(n_\pm \geqslant 6)$	40	4.5 ± 1.0	5.1 ± 2.1
6. $\pi^-p \to \pi\pi X$	11.2	1.04 ± 0.1	0.41 ± 0.15
7. $\pi^-C \to p2\pi^-\pi^+X$	3.7	2.6 ± 1.2	0.76 ± 0.47
8. $\bar{p}p \to \pi\pi X$ $(n_\pm \geqslant 6)$	22.4	$R_\parallel = 4.4\pm1.4$ $R_\perp = 1.7\pm0.4$	$c\tau_1 = 1.4\pm0.5$ $c\tau_2 = 3.1\pm1.6$
9. $\pi^+p \to \pi\pi X$ $(n_\pm \geqslant 6)$	16	1.84 ± 0.06	1.1 ± 0.2
10. $K^-p \to \pi\pi X$ $(n_\pm \geqslant 6)$	16	1.84 ± 0.09	1.0 ± 0.2
11. $\bar{p}\bar{p} \to \pi\pi X$ $(n_\pm = 4)$	0.0	1.89 ± 0.06	1.5 ± 0.2
12. $\bar{p}p \to \pi\pi X$ $(n_\pm = 4)$	5.7	2.2 ± 0.2	2.9 ± 0.6
13. $K^-p \to \pi\pi X$ $(n_\pm = 6.8$	12.0	1.9 ± 0.3	—
14. $pp \to \pi\pi X$	$\sqrt{s} = 53$ GeV	1.34 ± 0.31	1.38 ± 0.60

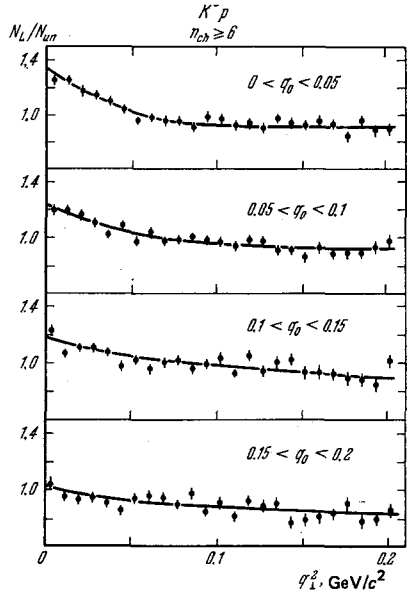

FIG. 29. Ratio of the yields of pairs of identical and nonidentical pions as a function of q_1^2 for K^-p interactions at $p = 16$ GeV/c. The curves are an approximation of the data by the equation

$$\frac{N_L}{N_{un}} = C(1+\lambda\Delta);$$

where N_L/N_{un} is the ratio of $N(\pi^\pm\pi^\pm)$ to $N(\pi^+\pi^-)$.

and that it is two-dimensional. The actual values found for R and τ, however, must be judged preliminary at this point, for the following reasons. First, the ratio W/W_0 in the limits $q_1^2 \to 0$ and $q_0 \to 0$ is usually less than two, but this is not what we would expect on the basis of Eq. (5.3). There are many possible reasons for this discrepancy, e.g., the use of $\pi^+\pi^-$ combinations as a background. There are no interference correlations for these combinations in the simple statistical models, but in the multiperipheral models or in inclusive production of resonances there are such correlations. In all cases, the value of τ has turned out to be quite small. Since one of the components of τ is of a geometric nature,[84] the actual lifetime is even shorter, and this result is difficult to reconcile with the statistical models. Furthermore, the calculations of the errors in the determination of R and τ have not taken into account the uncertainty in the choice of the background distribution.

Notwithstanding all these comments, the quantity R is apparently a weak function of the nature and energy of the primary particles.[26)]

In principle, correlation analysis can also tell us about the shape of the emission region; this analysis would be based, for example, on pairs of pions which are emitted in the forward direction ($|\cos\theta| \geq 0.5$) and at a large angle ($|\cos\theta| \leq 0.5$) in the c.m. system. Attempts have been made to carry out the corresponding measurements for π^-p and pp interactions and for $\bar{p}p$ collisions.[26,88,89] In both cases, evidence of a deviation from a sphere was found, but in the former case the ellipsoid is compressed along the direction of the primary particles, while in the latter case it is stretched out in this direction (Table VII). This question clearly deserves further study.

Interference of identical particles has thus been observed experimentally in multiple-production processes. The dimensions of the region from which the secondary pions are emitted have turned out to be $(1-2)\cdot 10^{-13}$ cm, and the lifetime of the excited states has turned out to be $\tau \sim 10^{-23}$ sec. These "average" characteristics, however, are governed by the combination of many hadron-production mechanisms in strong interactions. The production of resonances is important here[87,89] (Section 4). The next step would thus be to study the interference of resonances (for example, $\rho\rho$ and $\omega\omega$), and these experiments will not be simple (Subsection 4a). From the standpoint of the quark-parton models we need to study the dimensions of the hadron-emission region as a function of the hadron momenta (Subsection 4d). It would be particularly interesting to study the interference of identical particles for processes in which particles are produced with large transverse momenta, in which we would expect the quark-quark interaction to be predominant. Answers to these questions must await correlation experiments with various "sets" of primary particles in the accelerator energy range for long-lived secondary particles (π, K, N, $\bar{N}$, Λ, etc.) and resonances. It is also clear from the data available that the statistical base must be increased by one or two orders of magnitude. It is accordingly necessary to make widespread use of electronic methods specially "tuned" to search for interference.

6. CONCLUSION

Inclusive processes in hadron interactions have been under study now for 30 years. The first experiments in this direction (1948–1968) were carried out with cosmic rays, and these experiments revealed the first general aspects of multiple-production processes.[16,19] Among these general aspects are a limitation on the transverse momenta of the secondary particles and the associated peripheral nature of the hadron collisions. These aspects have played an important role in our study of the nature of strong interactions. A new stage in this field of research began with the appearance of accelerators with $E = 70-2000$ GeV (Serpukhov, Geneva, and Batavia), which have made possible a detailed study of multiple-production processes at high energies. These processes constitute $\approx 80\%$ of all hadron interactions. New methods for studying many-particle reactions (the inclusive approach)[14,15] and new ideas regarding hadron structure[8] have brought us much closer to an understanding of the nature of strong interactions.

Let us summarize what has been learned about inclusive processes in hadron interactions in accelerator-based research from 1968 to 1978. We will begin with the experimental information.

1) The average secondary-particle multiplicities

[26)] Exceptions are $\bar{p}p$ and $\pi^{-12}C$ interactions.

have been studied as a function of the energy over the energy range 10–200 GeV (Section 2). It turns out that the average multiplicity increases slowly [$\langle n_\pm \rangle \sim (\ln s)^n$ with $n = 1-2$, or a weak power-law increase].

2) The multiplicity distributions conform to scaling with respect to the variable $n/\langle n \rangle$, and they depend slightly on the energy and nature of the primary hadron (Subsection 2b).

3) Correlations have been observed in the multiplicities for different types of hadrons (pions and kaons; Subsection 2b).

4) Study of one-particle inclusive spectra of hadrons in reactions $ab \to cX$ has shown that there are two regions of multiple production (the central region and the fragmentation region), in which different mechanisms are operating to produce the particles (Section 3).

5) In the fragmentation region, a new type of strong-interaction symmetry has been established for exotic reactions: scaling at $E \gtrsim 20$ GeV. On the other hand, there is a pronounced deviation from scaling for the production of particles such as π, K, and $\bar{p}$ in the central region ($x \approx 0$) up to $E = 2000$ GeV (Section 3).

6) Study of two-particle correlations in the process $ab \to c_1 c_2 X$ has shown that there are short-range correlations between secondary hadrons ($L \approx 2$) (Section 3). The same reactions have demonstrated interference of identical particles with approximately equal momenta, and this interference is now used widely as a tool for studying the dimensions of the region from which the secondary hadrons are emitted (Section 5).

7) The most important recent achievement has been the discovery that resonances constitute a large fraction of the products in multiple-production processes (≈80–90%). The fraction of pions which are formed directly in hadron interactions is estimated to be some 6–20% (Section 4).

8) In first approximation, the distributions of resonances with respect to longitudinal and transverse momenta in the central region are independent of the nature of the resonances and the nature of the primary particles in the energy range $E = 10-24$ GeV. The distributions of resonances with respect to transverse momenta are described by a function $(-Bp_\perp^2)$ with $B \approx 3.4$ $(\text{GeV}/c)^{-2}$ for $p_\perp^2 = 0-2$ $(\text{GeV}/c)^2$ and $M = 0.5-1.4$ GeV (Subsection 4c).

Those pions which are not products of the decay of resonances vary with $p_\perp^2$ in the same way. In this connection, the nature of the increase in $\langle p_\perp \rangle$ with increasing M, which was discovered in the 1950s, has now been clarified. This behavior is now explained on the basis of the kinematics of the decay of resonances (Subsection 4c).

9) A new and surprising fact is that the distributions of particles (p, π, K, Λ), resonances (ρ, ω) at $|y| \lesssim 1.0$, and systems of uncorrelated pions $(2\pi, 3\pi, 4\pi)$ can be described satisfactorily by a function of the type $\exp(-E_\perp/T)$, where T is the effective temperature of the hadron matter, which remains essentially constant over a broad energy range (10–2000 GeV) and has the value $T \sim m_\pi (1/T \sim 7\ \text{GeV}^{-1})$ (Subsection 4c).

It is extremely probable that Eqs. (4.9) and (4.10) are consistent because of the large errors in the experimental determination of $d\sigma(R)/dp_\perp^2$, since $Bp_\perp^2 = B[E_\perp - M(R)][E_\perp + M(R)] \approx 7(E_\perp - M)$. For the kaons, however, and especially for the pions, which are the primary products of resonance decay, the thermodynamic description is surprising. A resolution of this problem should be expected after a refinement of the experimental data (Subsection 4c).

10) The characteristics of multiple-production processes in the central region have been found to be essentially independent of the nature of the primary hadrons. Furthermore, the behavior of $\langle n(s) \rangle$ for the weak, electromagnetic, and strong interactions is governed primarily by the total energy which is expended on hadron production, rather than by the nature of the interaction ($\sqrt{s} \lesssim 10-20$ GeV). However, experiments on multiple production using existing accelarators are far from completion. We do not have enough data on $\langle n_i \rangle = f(s)$ and $\langle n_i^R \rangle = f(s)$ for the various types of primary and secondary particles. Data on one-particle and two-particle inclusive processes are not available over the entire energy range. Finally, information on resonance production is available only for certain energies ($E \gtrsim 20$ GeV). The discovery of the two-step (or multistep) nature of multiple-production processes ($ab \to RX, R \to cd$) will undoubetedly cause a large-scale study of many-particle reactions in which those hadrons which are produced immediately in the collisions of the primary particles are distinguished.

The theory which is available for multiple-production processes spans a broad range from hydrodynamic models to quark-parton models.[17-20,23] Each model can describe certain features of the inclusive reactions. The models which have been developed most thoroughly, to the point at which a quantitative comparison with experiment is possible, are the statistical-hydrodynamic and multiperipheral models, which are reviewed in Ref. 23. Accordingly, we have simply emphasized a new tendency in the development of quark models, stemming from the discovery of intense resonance production. This approach is attractive because it promises a common description of the mass spectrum of the hadrons and their statistical properties and the dynamics of multiple-production processes in weak, electromagnetic, and strong interactions on the basis of the quark structure of hadrons.[8,13] Confirmation of the universal behavior of the resonance spectra and of the dominant role of resonances in strong interactions,[13] predicted in 1973, raises the hope that this is the correct approach. On the other hand, the statistical nature of the secondary-hadron distributions in the central region shows that the statistical models also reflect certain aspects of multiple-production processes,[17,18,20] but it may be that they should be used at the "quark level." The multiperipheral models for strong interactions, which have made many quantitative predictions for inclusive processes,[20,23] undoubtedly also reflect the basic features of the quark-parton description.

It is thus clear that a theory for strong interactions must synthesize the most important features of these three approaches. Crucial to the development of this theory is new experimental information on multiple-production processes in weak, electromagnetic, and strong interactions at $\sqrt{s} \leqslant 60$ GeV. It would be particularly important to obtain information on hadrons which are not products of the decay of resonances or clusters. It can also be seen from the data available that important advances will be made when new accelerators open up the energy range $1-10^3$ TeV, presumably in 1981–1985.

This decade of accelerator research on inclusive reactions has thus proved extremely fruitful. Promising approaches to a theory of strong interactions and to the relationship between this theory and that for electromagnetic and weak interactions have been identified.[8,75,77,78] Theoretical predictions regarding the quark-parton structure of hadrons have been confirmed experimentally. It is expected that the quark structure of hadrons will become more apparent as the energy of the primary particles is increased. The development of a new generation of accelerators will clearly help physicists learn much about the structure of hadrons and the nature of strong interactions.

[1]M. A. Markov, Usp. Fiz. Nauk **111**, 719 (1973) [Sov. Phys. Usp. **16**, 913 (1974)].
[2]D. I. Blokhintsev *et al.*, Usp. Fiz. Nauk **109**, 259 (1973) [Sov. Phys. Usp. **16**, 82 (1973)].
[3]J. D. Bjorken, Fiz. Elem. Chastits At. Yadra **4**, 407 (1973).
[4]R. Jackiw, Phys. Today **25** (1), 23 (1972) [Russ. Transl., Usp. Fiz. Nauk **109**, 743 (1973)].
[5]T. D. Lee, Fiz. Elem. Chastits At. Yadra **4**, 689 (1973).
[6]V. A. Matveev, R. M. Muradyan, and A. N. Tavkhelidze, Fiz. Elem. Chastits At. Yadra **2**, 7 (1971); R. M. Muradyan, Preprint R2-6762, Joint Institute for Nuclear Research, Dubna, 1972.
[7]N. N. Bogolyubov, V. S. Vladimirov, and A. N. Tavkhelidze, Teor. Mat. Fiz. **12**, 305 (1972).
[8]R. P. Feynman, Photon-Hadron Interactions Benjamin, New York (1972) [Russ. Transl., Mir, Moscow, 1975].
[9]R. P. Feynman, Phys. Rev. Lett. **23**, 1415 (1969).
[10]J. Benecke *et al.*, Phys. Rev. **188**, 2159 (1969); T. T. Chou and C. N. Yang, Phys. Rev. Lett. **25**, 1072 (1970).
[11]B. Feld, Models of Elementary Particles, Blaisdell, Waltham, Mass., 1969 (Russ. Transl., Mir, Moscow, 1971); V. De Alfero *et al.*, Currents in Hadron Physics, American Elsevier, New York, 1973 (Russ. Transl., Mir, Moscow, 1976).
[12]H. W. Kendall and W. K. H. Panofsky, Sci. Am. **224** (6), 60 (1971) [Russ. Transl., Usp. Fiz. Nauk **106**, 315 (1972)]; S. D. Drell, Comm. Nucl. Part. Phys. **4**, 147 (1970) [Russ. Transl., Usp. Fiz. Nauk **106**, 331 (1972)].
[13]V. V. Anisovich and V. M. Shekhter, Nucl. Phys. Ser. B **55**, 455 (1973); E. M. Levin and M. G. Ryskin, Yad. Fiz. **17**, 388 (1973) [Sov. J. Nucl. Phys. **17**, 199 (1973)]; Phys. Lett. Ser. B **41**, 626 (1977).
[14]A. A. Logunov and M. A. Mestvirishvili, Preprint D1, 2-7411, Joint Institute for Nuclear Research, Dubna, 1973, p. 376.
[15]A. A. Logunov *et al.*, Phys. Lett. Ser. B **25**, 611 (1967).
[16]V. M. Murzin and L. I. Sarycheva, Kosmicheskie luchi i ikh Vzaimodeĭstvie (Cosmic Rays and Their Interactions), Atomizdat, Moscow, 1968.
[17]E. L. Feĭnberg, Phys. Rept. **C5**, 237 (1972).
[18]E. L. Feĭnberg, Usp. Fiz. Nauk **104**, 539 (1971) [Sov. Phys. Usp. **14**, 455 (1972)].
[19]V. S. Murzin and L. I. Sarychev, Mnoshestvennye protsessy pri vysokikh energiyakh (High-Energy Multiple-Production Processes), Atomizdat, Moscow, 1974.
[20]Yu. P. Nikitin and I. L. Rozental', Teoriya mnozhestvennykh protsessov (Theory of Multiple-Production Processes), Atomizdat, Moscow, 1976; Yu. P. Nikitin, I. L. Rozental', and F. M. Sergeev, Usp. Fiz. Nauk **121**, 3 (1977) [Sov. Phys. Usp. **20**, 1 (1977)].
[21]V. G. Grishin, Fiz. Elem. Chastits At. Yadra **7**, 595 (1976) [Sov. J. Part. Nucl. **20**, 1 (1977)]; Trudy XVIII Mezhdunarodnoĭ konferentsii po fizike vysokikh energiĭ (Tbilisi-76) [Proceedings of the Eighteenth International Conference on High-Energy Physics (Tbilisi-76)], JINR, Dubna; Report D1-2-10400, Joint Institute for Nuclear Research, Dubna, 1977, A2-6.
[22]A. K. Likhoded and P. V. Shlyapnikov, Usp. Fiz. Nauk **124**, 3 (1978) [Sov. Phys. Usp. **21**, 1 (1978)].
[23]I. V. Andreev and I. M. Dremin, Usp. Fiz. Nauk **122**, 37 (1977) [Sov. Phys. Usp. **20**, 381 (1977)]; I. M. Dremin and C. Quigg, Usp. Phys. Nauk **124**, 535 (1978) [Sov. Usp. **21**, 265 (1978)].
[24]A. B. Kaĭdalov, Cited in Paper A1-27, Proceedings of the Eighteenth International Conference on High-Energy Physics (Tbilisi-76), JINR, Dubna.
[25]A. Wroblewski, in: Proc. of Eighth Intern. Symposium on Multiparticle Dyanamics, Kaysersberg, France, 1977, A-1.
[26]A. Zieminski, in: Proc. of the 1977 European Conference on Particle Physics, Budapest, 1977, p. 163.
[27]W. Thomé *et al.*, Nucl. Phys. Ser. B **129**, 365 (1977).
[28]Z. Koba, H. Nielsen, and P. Olesen, Nucl. Phys. Ser. B **40**, 317, 633 (1972).
[29]A. Wroblewski, Acta Phys. Polonica. Ser. B **4**, 857 (1973); A. Buras and Z. Koba, Nuovo Cimento Lett. **6**, 629 (1973).
[30]A. J. Buras *et al.*, Phys. Lett. Ser. B **47**, 251 (1973).
[31]E. M. Levin and M. G. Ryskin, Yad. Fiz. **19**, 669 (1974) [Sov. J. Nucl. Phys. **19**, 338 (1974)].
[32]L. Van Hove, Phys. Lett. Ser. B **43**, 63 (1973).
[33]N. S. Angelov *et al.*, Yad. Fiz. **21**, 166, 1298 (1975) [Sov. J. Nucl. Phys. **21**, 87 (1975)].
[34]V. G. Grishin and P. P. Kerachev, Yad. Fiz. **22**, 579 (1975) [Sov. J. Nucl. Phys. **22**, 300].
[35]A. U. Abdurakhimov *et al.*, Yad. Fiz. **16**, 689 (1972) [Sov. J. Nucl. Phys. **16**, 386 (1973)]; **17**, 1235 (1973) [**17**, 644 (1973)].
[36]K. Jaeger *et al.*, Phys. Rev. **D11**, 2405 (1975).
[37]V. G. Grishin *et al.*, Yad. Fiz. **17**, 1281 (1973) [Sov. J. Nucl. Phys. **17**, 667 (1973)]; A. N. Sisakyan and L. A. Slepchenko, Preprint R2-10651, Joint Institute for Nuclear Research, Dubna, 1977.
[38]E. M. Levin and M. G. Ryskin, Yad. Fiz. **20**, 519 (1974) [Sov. J. Nucl. Phys. **20**, 280 (1975)].
[39]M. Derrick *et al.*, Phys. Rev. **D17**, 1 (1978).
[40]K. Guettler *et al.*, Nucl. Phys. Ser. B **116**, 77 (1976).
[41]I. M. Dremin *et al.*, Zh. Eksp. Teor. Fiz. **48**, 952 (1965) [Sov. Phys. JETP **21**, 633 (1965)]; Usp. Fiz. Nauk **101**, 385 (1970) [Sov. Phys. Usp. **13**, 438 (1971)].
[42]E. I. Volkov *et al.*, Yad. Fiz. **18**, 437 (1973) [Sov. J. Nucl. Phys. **18**, 226 (1974)]; **20**, 149 (1974) [**20**, 78 (1975)].
[43]E. I. Volkov *et al.*, Yad. Fiz. **24**, 1212 (1976) [Sov. J. Nucl. Phys. **24**, 635 (1976)].
[44]J. Derre *et al.*, Phys. Lett. Ser. B **50**, 287 (1974).
[45]K. Singer *et al.*, Phys. Lett. Ser. B **49**, 481 (1974).
[46]J. Ranft, in: Proc. of the Fifth Intern. Symposium on Many Particle Hydrodynamics, Leipzig, 1974, p. 210.
[47]M. Le Bellack, in: Proc. of the Seventh Intern. Colloquium on Multiparticle Reactions, München, 1976, p. 1.
[48]N. Angelov *et al.*, Yad. Fiz. **22**, 122 (1975) [Sov. J. Nucl. Phys. **22**, 59 (1975)]; **24**, 83 (1976) [**24**, 41 (1976)]; Preprint R1-10177, Joint Institute for Nuclear Research, Dubna, 1976.

[49]W. D. Shepard, Cited in Proc. of the Seventh Intern. Colloquium on Multiparticle Reactions, München, 1976, p. 42.
[50]A. R. Erwin *et al.*, Phys. Rev. **D14**, 2219 (1976).
[51]N. N. Biswas *et al.*, Phys. Rev. Lett. **37**, 175 (1976).
[52]M. I. Adamovich *et al.*, Nuovo Cimento, Ser. A **33**, 183 (1976).
[53]V. A. Belyakov, V. I. Veksler, *et al.*, Zh. Eksp. Teor. Fiz. Fiz. **46**, 1967 (1964) [Sov. Phys. JETP **19**, 1326 (1964)].
[54]N. S. Angelov *et al.*, Preprint R1-9536, Joint Institute for Nculear Research, Dubna, 1976.
[55]N. S. Angelov *et al.*, Preprint R1-9810, Joint Institute for Nuclear Research, Dubna, 1977; Yad. Fiz. **25**, 117 (1977) [Sov. J. Nucl. Phys. **25**, 63 (1977)].
[56]N. S. Angelov *et al.*, Preprint R1-10616, Joint Institute for Nuclear Research Dubna, 1977.
[57]G. Jancso *et al.*, Nucl. Phys. Ser. B **124**, 1 (1977).
[58]W. Kittel, Cited in: Proc. of Eighth Intern. Symposium on Multiparticle Dynamics, Kaysersberg, France, 1977, A-81.
[59]V. M. Shekhter and L. M. Shcheglova, Preprint LNP1381, Leningrad, 1977.
[60]Yu. M. Antipov *et al.*, Preprint IHEP 76-42, Serpukhov, 1976.
[61]M. Binkley *et al.*, Phys. Rev. Lett. **37**, 571, 574 (1976).
[62]J. Bartke *et al.*, Nucl. Phys. Ser. B **120**, 14 (1977).
[63]M. Deutschmann *et al.*, Nucl. Phys. Ser. B **70**, 189 (1974).
[64]B. Alper *et al.*, Nucl. Phys. Ser. B **87**, 19 (1975).
[65]M. Ta-chung and E. Moeller, Phys. Rev. **D14**, 1449 (1976).
[66]E. L. Feĭnberg, Preprint 172, Lebedev Physics Institute, Moscow, 1976.
[67]I. Ya. Pomeranchuk, Dokl. Akad. Nauk SSSR **78**, 889 (1961); E. L. Feĭnberg, Usp. Fiz. Nauk **104**, 539 (1971) [Sov. Phys. Usp. **14**, 455 (1972)].
[68]V. M. Shekhter, in: Materialy XII zimneĭ shkoly LIYaF (Proceedings of the Twelfth Winter School of the Leningrad Institute of Nuclear Physics), LIYaF Akad. Nauk SSSR, Leningrad, 1977, p. 3.
[69]V. V. Anisovich and V. M. Shekhter, Preprint D1, 2-7411, Joint Institute for Nuclear Research, Dubna, 1973, p. 428.
[70]V. M. Shekhter, Preprint D1, 2-9224, Joint Institute for Nuclear Research, Dubna, 1975, p. 277.
[71]Yu. I. Shabel'skiĭ, in: Materialy XIII zimneĭ shkoly LIYaF (Proceedings of the Thirteenth Winter School of the Leningrad Institute of Nuclear Physics), LIYaF Akad. Nauk SSSR, Leningrad, 1978, p. 90; V. V. Anisovich *et al.*, Nucl. Phys. Ser. B **133**, 477 (1978).
[72]E. M. Levin and L. L. Frankfurt, Pis'ma Zh. Eksp. Teor. Fiz. **2**, 105 (1965) [JETP Lett. **2**, 65 (1965)].
[73]J. J. J. Kokkedee and L. Van Hove, Nuovo Cimento **42**, 711 (1966).
[74]J. W. Elbert *et al.*, Phys. Rev. **D3**, 2042 (1971).
[75]L. Van Hove, Usp. Fiz. Nauk **124**, 509 (1978) [Sov. Phys. Usp. **21**, 252 (1978)].
[76]N. S. Angelov *et al.*, Yad. Fiz. **26**, 811 (1977) [Sov. J. Nucl. Phys. **26**, 426 (1977)].
[77]A. I. Vaĭnshtein *et al.*, Usp. Fiz. Nauk **123**, 217 (1977) [Sov. Phys. Usp. **20**, 796 (1977)].
[78]Yu. L. Dokshtiser *et al.*, in: Collection, see Ref. 21.
[79]R. Hanbury Brown and R. Q. Twiss, Phil. Mag. **45**, 663 (1954).
[80]G. Goldhaber *et al.*, Phys. Rev. **120**, 300 (1960).
[81]V. G. Grishin, G. I. Kopylov, and M. I. Podgoretskiĭ, Yad. Fiz. **13**, 1116 (1970) [Sov. J. Nucl. Phys. **13**, 638 (1971)]; **14**, 600 (1971) [**14**, 335 (1972)].
[82]G. I. Kopylov and M. I. Podgoretskiĭ, Zh. Eksp. Teor. Fiz. **69**, 414 (1975) [Sov. Phys. JETP **42**, 211 (1975)].
[83]G. I. Kopylov and M. I. Podgoretskiĭ, Preprint D1, 2-7411, Joint Institute for Nuclear Research, Dubna, 1973, p. 483.
[84]M. I. Podgoretskiĭ, Preprint D1, 2-10400, Joint Institute for Nuclear Research, Dubna, 1977, A2-27.
[85]G. I. Kopylov and M. I. Podgoretskiĭ, Yad. Fiz. **15**, 392 (1972) [Sov. J. Nucl. Phys. **15**, 219 (1972)]; **18**, 656 (1973) [**18**, 336 (1974)]; **19**, 434 (1974) [**19**, 215 (1974)].
[86]G. Cocconi, Phys. Lett. Ser. B **49**, 459 (1974).
[87]P. Grassberger, Nucl. Phys. Ser. B **120**, 231 (1977).
[88]N. Angelov *et al.*, Yad. Fiz. **26**, 796 (1977) [Sov. J. Nucl. Phys. **26**, 419 (1977)]; **27**, 675 (1978) [**27**, 361 (1978)].
[89]V. V. Filoppova *et al.*, Preprint JINR E1-11083, Joint Institute for Nuclear Research, Dubna, 1977.
[90]Yu. D. Baiyukov *et al.*, Preprint ITEF-70, Institute of Theoretical and Experimental Physics, Moscow, 1976.
[91]A. V. Aref'ev *et al.*, Yad. Fiz. **27**, 716 (1978) [Sov. J. Nucl. Phys. **27**, 383 (1978)].

Translated by Dave Parsons